

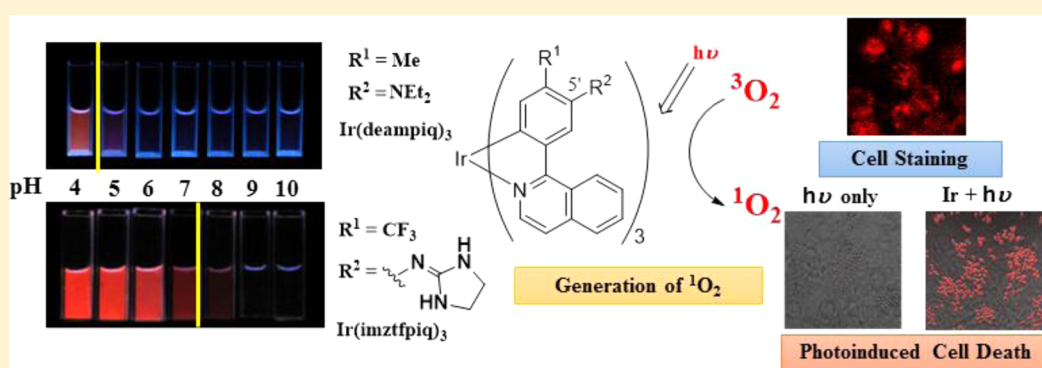
# Photochemical Properties of Red-Emitting Tris(cyclometalated) Iridium(III) Complexes Having Basic and Nitro Groups and Application to pH Sensing and Photoinduced Cell Death

Aya Kando,<sup>†</sup> Yosuke Hisamatsu,<sup>†</sup> Hiroki Ohwada,<sup>†</sup> Taiki Itoh,<sup>†</sup> Shinsuke Moromizato,<sup>†</sup> Masahiro Kohno,<sup>‡</sup> and Shin Aoki<sup>\*,†</sup>

<sup>†</sup>Faculty of Pharmaceutical Sciences, Tokyo University of Science, 2641 Yamazaki, Noda, Chiba 278-8510, Japan

<sup>‡</sup>Graduate School of Bioscience and Biotechnology, Tokyo Institute of Technology, 4259 Nagatsuta-cho, Midori-ku, Yokohama, Kanagawa 226-8503, Japan

## Supporting Information



**ABSTRACT:** Cyclometalated iridium(III) complexes, because of their photophysical properties, have the potential for use as luminescent probes for cellular imaging. We previously reported on a pH-activatable iridium complex that contains three *N,N*-diethylamino groups, namely, *fac*-Ir(deatpy)<sub>3</sub> **5**, which was synthesized via a regioselective aromatic substitution reaction at the 5'-position with tolylpyridine groups of *fac*-Ir(tpy)<sub>3</sub> **2**. It was found that **5** shows a considerable enhancement in emission intensity in the pH range from neutral to slightly acidic (pH 6.5–7.4) in aqueous solution and selectively stains lysosome in HeLa-S3 cells, due to the protonation of the diethylamino groups. In addition, **5** functions as a pH-dependent singlet oxygen (<sup>1</sup>O<sub>2</sub>) generator and induces necrosis-like cell death. However, observing the green emission of **5** is often hampered by autofluorescence emanating from nearby tissues. To overcome this problem, we designed and synthesized a series of new pH-activatable Ir(III) complexes that contain diethylamino, guanidyl, and iminoimidazolidinyl groups on the mpiq ligand of Ir(mpiq)<sub>3</sub> **7** and the tfpiq ligand of Ir(tfpiq)<sub>3</sub> **8**, which exhibit a red emission, namely, Ir(deampiq)<sub>3</sub> **13**, Ir(gmpiq)<sub>3</sub> **14**, Ir(imzmpiq)<sub>3</sub> **15**, and Ir(imztfpiq)<sub>3</sub> **16**. The emission intensity of these Ir complexes is enhanced substantially by protonation of their basic groups, and they induce the necrosis-like cell death of HeLa-S3 cells by photoirradiation at 465 nm. A strong orange-red emission of Ir(mpiq-NO<sub>2</sub>)<sub>3</sub> **9** and Ir(tfpiq-NO<sub>2</sub>)<sub>3</sub> **10** is also reported.

## INTRODUCTION

Intracellular pH plays a key role in various biological processes, and pH-activatable probes<sup>1</sup> can be useful tools for monitoring intracellular pH and cancer tissues, the pH of which is slightly acidic in comparison with that of normal tissues.<sup>2</sup> A number of fluorescent pH probes have been reported, and some of them are now commercially available (e.g., LysoSensor, Blue DND-167, and SNARF-5F).<sup>1</sup> As representative examples, Urano and co-workers demonstrated highly specific in vivo cancer visualization by using pH-activatable BODIPY dyes bearing a cancer-targeting monoclonal antibody.<sup>3</sup>

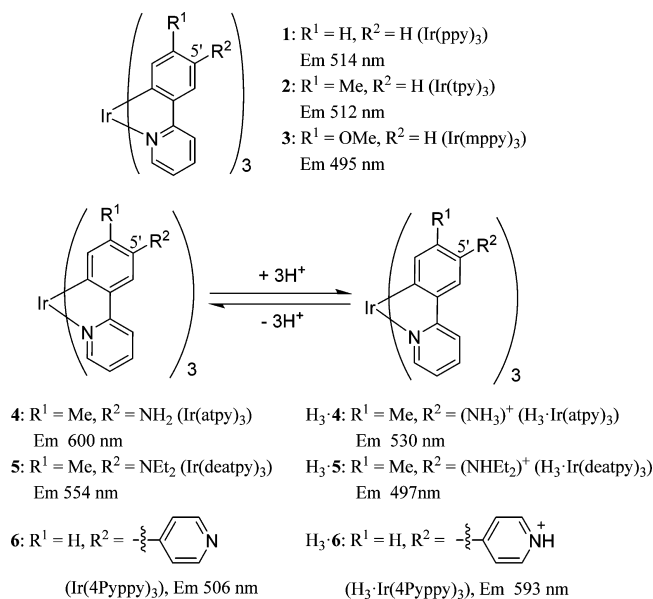
Meanwhile, cyclometalated iridium(III) complexes have received considerable attention due to their high phosphorescent quantum yields, excellent color-tuning capability, larger Stokes' shifts, and relatively longer lifetimes ( $\tau$  on the order of microseconds)

compared to fluorescent molecules ( $\tau$  on the order of nanoseconds).<sup>4</sup> These attractive properties make them promising and important candidates, not only for use in organic light emitting diodes (OLEDs) as phosphorescent emitters<sup>5</sup> but also for biological applications such as chemosensors,<sup>6</sup> cellular imaging probes,<sup>7</sup> in vivo tumor imaging,<sup>8</sup> and photosensitizers for the production of singlet oxygen (<sup>1</sup>O<sub>2</sub>).<sup>9</sup> Although some pH-responsive Ir complexes have been reported so far,<sup>10</sup> applications of them to cellular imaging remain limited.<sup>10c,g,h</sup>

We recently reported on the regioselective halogenation, nitration, and formylation of phenylpyridine-type tris(cyclometalated)

Received: February 17, 2015

Chart 1



Ir complexes (e.g., *fac*-Ir(ppy)<sub>3</sub> **1** (ppy = 2-phenylpyridine), *fac*-Ir(tpy)<sub>3</sub> **2** (tpy = 2-(4'-tolyl)pyridine), and **3** (mppy = 2-(4'-methoxyphenyl)pyridine); see Chart 1) at the 5'-position (R<sup>2</sup> at the *p*-position with respect to the C–Ir bond) of the phenyl rings and their subsequent conversion to amino, cyano, and sulfonyl Ir complexes that exhibit a blue-red-color emission.<sup>11,12</sup> Among these analogues, *fac*-Ir(atpy)<sub>3</sub> **4** (atpy = 2-(5'-amino-4'-tolyl)pyridine) containing three amino groups was found to show a weak red emission at ca. 600 nm in the neutral–alkaline pH range and a green emission (at ca. 530 nm) at pH < 5, due to the protonation of its amino groups (Chart 1).<sup>11a</sup> The tris-(diethylamino) derivative Ir(deatpy)<sub>3</sub> **5** (deatpy = 2-(5'-*N,N*-diethylamino-4'-tolyl)pyridine) functions as pH-activatable probe that exhibits a considerable change in emission intensity between neutral and slightly acidic pH (pH 6.5–7.4).<sup>11c</sup> On the other hand, the emission characteristics of Ir(4Pyppy)<sub>3</sub> **6** (4Pyppy = 2-(5'-(*p*-pyridyl)phenyl)pyridine), which contain pyridyl groups at the 5'-position of the 2-phenylpyridine (ppy) ligand, are opposite to that for **4**.<sup>11d</sup> Namely, the green-colored emission (at ca. 500 nm) of **6** changes to red (at ca. 590 nm) when the three pyridyl groups are protonated.<sup>11d</sup> The results of a cellular imaging study of HeLa-S3 cells indicate that **5** could be useful for the selective staining of lysosomes, which are acidic organelles that are located in cells, and that **6** could be used to stain mitochondria, whose pH is ca. 7.5. Also note that **5** and **6** are able to induce cell death when photoirradiated with UV light.<sup>11c,d</sup> However, the actual visualization of their green emission is often hampered by autofluorescence from nearby living cells and tissues, and the use of less toxic visible light would be preferable for the photochemical induction of cell death.

To overcome these problems, we designed and synthesized the amino, diethylamino, guanidyl, and iminoimidazolidinyl derivatives of *fac*-Ir(mpiq)<sub>3</sub> **7**<sup>13</sup> (mpiq = 1-(4'-methylphenyl)isoquinoline) and *fac*-Ir(tfpiq)<sub>3</sub> **8** (tfpiq = 1-(4'-trifluoromethylphenyl)isoquinoline) that exhibit a red emission (at ca. 600 nm). The examples include **11** (Ir(ampiq)<sub>3</sub>, ampiq = 1-(5'-amino-4'-methylphenyl)isoquinoline), **12** (Ir(atfpiq)<sub>3</sub>, atfpiq = 1-(5'-amino-4'-trifluoromethylphenyl)isoquinoline), **13** (Ir(deampiq)<sub>3</sub>, deampiq = 1-(5'-diethylamino-4'-methylphenyl)isoquinoline), **14** (Ir(gmpiq)<sub>3</sub>, gmpiq = 1-(5'-guanidyl-4'-methylphenyl)isoquinoline),

**15** (Ir(imzmpiq)<sub>3</sub>, imzmpiq = 1-(5'-iminoimidazolidinyl-4'-methylphenyl)isoquinoline) and **16** (Ir(imztfpiq)<sub>3</sub>, imztfpiq = 1-(5'-iminoimidazolidinyl-4'-trifluoromethylphenyl)isoquinoline). Prior to the synthesis, the pK<sub>a</sub> values of these derivatives were predicted based on the pK<sub>a</sub> values of the corresponding aniline derivatives using the SciFinder database. It was revealed that the emission of **11** and **13** changes at a pH below 6, which is lower than that of Ir(deatpy)<sub>3</sub> **5**, and that the pK<sub>a</sub> values of **14** and **15** (ca. 8–9) are higher than that of **5**. Finally, we succeed in the synthesis of **16** Ir(imztfpiq)<sub>3</sub>, which has a pK<sub>a</sub> value of 7, by the introduction of three iminoimidazolidinyl groups to the trifluoromethyl analogue **8**. We report herein on the synthesis and pH-dependent photophysical behaviors of these Ir complexes, the generation of singlet oxygen (<sup>1</sup>O<sub>2</sub>), and the induction of cell death by photoirradiation with visible light. We also report on the strong orange-red emission of **9** and **10**, which are nitro derivatives of **7** and **8**.

## EXPERIMENTAL SECTION

**General Information.** IrCl<sub>3</sub>·3H<sub>2</sub>O and ethyl iodide were purchased from Kanto Chemical Co. 10% Pd/C, 1,3-diphenylisobenzofuran (DBPF), and carbonyl cyanide 3-chlorophenylhydrazone (CCCP) were purchased from Sigma-Aldrich. Imidazolidine-2-thione, NaN<sub>3</sub>, propidium iodide (PI), and organic solvent for spectroscopic analyses were purchased from Wako Chemicals Co., Ltd. MEM (Gibco Minimum Essential Medium), MitoTracker Green FM, and LysoTracker Green DND-26 were purchased from Invitrogen. All aqueous solutions were prepared using deionized water. All synthetic procedures were performed under an atmosphere of argon. Negligible hazard exists in all synthetic procedures. Melting points were measured on a Yanaco MP-33 Micro melting point apparatus and are uncorrected. IR spectra were recorded on a PerkinElmer FTIR-Spectrum 100 (ATR). <sup>1</sup>H NMR (300 MHz) spectra were recorded on a JEOL Always 300 spectrometer. Electrospray ionization (ESI) mass spectra (MS) were recorded on Varian 910-MS. Thin-layer (TLC) and silica gel column chromatographies were performed using Merck 5554 (silica gel) TLC plates and Fuji Silysia Chemical FL-100D, respectively. Alumina (Al<sub>2</sub>O<sub>3</sub>) column chromatography was performed using Aluminum oxide 90 active neutral (Merck). Gel permeation chromatography (GPC) experiments were performed using a system consisting of a PONM P-50 (Japan Analytical Industry Co., Ltd.), a UV-vis detector S-3740 (Soma Japan), a Manual Sample Injector 7725i (Rheodyne, USA) and a MDL-101 1 pen recorder (Japan Analytical Industry Co., Ltd.), equipped with two GPC columns, Jaigel-1H and jaigel-2 (Japan Analytical Industry Co., Ltd., 20φ × 600 mm, Nos. A605201 and A605214). For measurement of luminescence spectra in aqueous solutions at given pH values, buffer solutions (CAPS, pH 11.0 and 10.0; CHES, pH 9.0; EPPS, pH 8.0; HEPES, pH 7.4 and 7.0; MES, pH 6.0, 5.0, and 4.0), citric acid–sodium citrate buffer (pH 3) and HCl–KCl buffer (pH 2.5, 2, and 1.0) were used. The Good's buffer reagents (Dojindo) were obtained from commercial sources: 2-morpholinoethanesulfonic acid (MES, pK<sub>a</sub> = 4.8), 2-[4-(2-hydroxyethyl)-1-piperazinyl]ethanesulfonic acid (HEPES, pK<sub>a</sub> = 7.5), 3-[4-(2-hydroxy-ethyl)-1-piperazinyl]propanesulfonic acid (EPPS, pK<sub>a</sub> = 8.0), 2-(cyclohexylamino)ethanesulfonic acid (CHES, pK<sub>a</sub> = 9.5), 3-cyclohexylamino-1-propanesulfonic acid (CAPS, pK<sub>a</sub> = 10.4). Emission lifetimes were determined using a TSP-1000 (Unisoku Co., Ltd.). Inductively coupled plasma atomic emission spectrometry (ICP–AES) measurements were performed on a Shimadzu ICPE-9000. Density functional theory (DFT) calculations were also performed using the Gaussian09 program (B3LYP, the LanL2DZ basis set for a Ir atom and the 6-31G basis set for H, C, F, O, and N atoms).<sup>14,15</sup> Microwave reactions were conducted using the Discover Bench Mate microwave apparatus and the corresponding vials. The reaction was performed in glass vials (capacity 10 mL) sealed with a septum, under magnetic stirring. The temperature of the reaction mixture was monitored using a calibrated infrared temperature control mounted under the reaction vial.

**Improved Method for the Synthesis of *fac*-Tris[1-(4'-methylphenyl)isoquinoline]iridium(III) (Ir(mpiq)<sub>3</sub>) (**7**).**<sup>13</sup> A solution

of 17 (1.00 g, 4.56 mmol), Na<sub>2</sub>SO<sub>4</sub> (648 mg, 4.56 mmol), and IrCl<sub>3</sub>·3H<sub>2</sub>O (53.6 mg, 0.15 mmol) in dioxane/H<sub>2</sub>O (1/1, 8 mL) was added to a microwave vial. The reactor was subjected to microwave irradiation at 150 °C for 50 min. After adding 30 mL of water, the solution was extracted with CHCl<sub>3</sub> (30 mL × 3). The combined organic layer was concentrated under reduced pressure, to which Na<sub>2</sub>SO<sub>4</sub> (648 mg, 4.56 mmol) and dioxane/H<sub>2</sub>O (1/1, 8 mL) were added, and the resulting mixture was microwave-irradiated at 150 °C to 50 min. After this procedure was repeated once more, the mixture was concentrated under reduced pressure. After adding 20 mL of water, the solution was extracted three times with CHCl<sub>3</sub> (30 mL). The combined organic layer was dried over Na<sub>2</sub>SO<sub>4</sub>, filtered, and concentrated under reduced pressure, and the resulting residue was purified by silica gel column chromatography (hexanes/CHCl<sub>3</sub> = 2:1) and recrystallization from hexanes/CH<sub>2</sub>Cl<sub>2</sub> to afford 7 as a red powder (63.8 mg, 50% yield).

**1-(4'-Trifluoromethylphenyl)isoquinoline (18).** 4-(Trifluoromethyl)phenylboronic acid (678 mg, 3.57 mmol) and Pd(PPh<sub>3</sub>)<sub>4</sub> (100 mg, 86.5 μmol) were added to a solution of 1-chloroisoquinoline (292 mg, 1.78 mmol) in 20 mL of toluene/EtOH/2 N Na<sub>2</sub>CO<sub>3</sub> aq (2/1/1), and the solution was degassed by bubbling with argon gas for 15 min. The reaction mixture was heated at 70 °C for 3 h. After the mixture cooled to room temperature, the insoluble materials were removed by filtration. After adding 15 mL of H<sub>2</sub>O to the filtrate, the solution was extracted with AcOEt (30 mL × 3). The combined organic layer was dried over Na<sub>2</sub>SO<sub>4</sub>, filtered, and concentrated under reduced pressure, and the resulting residue was purified by silica gel column chromatography (hexanes/AcOEt, 50:1) and recrystallization from hexanes/AcOEt to afford 18 as a white powder (486 mg, 99% yield). mp > 300 °C. IR (ATR): ν = 1618, 1556, 1405, 1320, 1158, 1105, 1059, 1017, 831, 757, 702, 680, 609 cm<sup>-1</sup>. <sup>1</sup>H NMR (300 MHz, CDCl<sub>3</sub>/TMS): δ = 8.63 (d, J = 5.4 Hz, 1H), 8.03 (d, J = 8.4 Hz, 1H), 7.93 (d, J = 8.4 Hz, 1H), 7.87–7.77 (m, 4H), 7.77–7.67 (m, 2H), 7.58 (dd, J = 8.3, 1.5 Hz, 1H) ppm. ESI-MS (*m/z*): Calcd for C<sub>16</sub>H<sub>11</sub>F<sub>3</sub>N (M+H)<sup>+</sup>: 274.0838. Found: 274.0837. Anal. Calcd for C<sub>16</sub>H<sub>10</sub>F<sub>3</sub>N: C, 70.33; H, 3.69; N, 5.13. Found: C, 70.35; H, 3.31; N, 4.99.

**fac-Tris[1-(4'-trifluoromethylphenyl)isoquinoline]iridium(III) (Ir(tfpiq)<sub>3</sub>) (8).** A mixture of 18 (300 mg, 1.10 mmol), Na<sub>2</sub>SO<sub>4</sub> (150 mg, 1.07 mmol), and IrCl<sub>3</sub>·3H<sub>2</sub>O (12.9 mg, 36.6 μmol) in 5 mL of dioxane/H<sub>2</sub>O (1/1) was added to a microwave vial. The reactor was subjected to microwave irradiation at 150 °C for 50 min. After it cooled to room temperature, the mixture was concentrated under reduced pressure, 30 mL of water was added, and the resulting solution was extracted with CHCl<sub>3</sub> (30 mL × 3). The combined organic layer was concentrated under reduced pressure, to which Na<sub>2</sub>SO<sub>4</sub> (150 mg, 1.07 mmol) and 5 mL of dioxane/H<sub>2</sub>O (1/1) were added, and the resulting mixture was subjected to microwave irradiation at 150 °C to 50 min. After adding 20 mL of water, the solution was extracted with CHCl<sub>3</sub> (30 mL × 3). The combined organic layer was dried over Na<sub>2</sub>SO<sub>4</sub>, filtered, and concentrated under reduced pressure, and the resulting residue was purified by silica gel column chromatography (hexanes/CHCl<sub>3</sub>, 3:4) and recrystallization from hexanes/CH<sub>2</sub>Cl<sub>2</sub> to afford 8 as a red powder (22.2 mg, 60% yield). mp > 300 °C. IR (ATR): ν = 3061, 1558, 1448, 1380, 1318, 1269, 1159, 1111, 904, 815, 731, 707, 677, 646, 572 cm<sup>-1</sup>. <sup>1</sup>H NMR (300 MHz, CDCl<sub>3</sub>/TMS): δ = 8.98–8.84 (m, 3H), 8.23 (d, J = 8.4 Hz, 3H), 7.80 (m, 3H), 7.75–7.65 (m, 6H), 7.33 (d, J = 6.2 Hz, 3H), 7.29–7.14 (m, 6H), 7.07 (s, 3H) ppm. ESI-MS (*m/z*): Calcd for C<sub>48</sub>H<sub>27</sub>F<sub>9</sub>(<sup>191</sup>Ir)N<sub>3</sub> (M<sup>+</sup>): 1007.1662. Found: 1007.1647. Anal. Calcd for C<sub>48</sub>H<sub>27</sub>F<sub>9</sub>IrN<sub>3</sub>·0.25CH<sub>2</sub>Cl<sub>2</sub>: C, 56.25; H, 2.69; N, 4.08. Found: C, 56.65; H, 2.35; N, 4.24%.

**fac-Tris[1-(5'-nitro-4'-methylphenyl)isoquinoline]iridium(III) (Ir(mpiq-NO<sub>2</sub>)<sub>3</sub>) (9).** Cu(NO<sub>3</sub>)<sub>2</sub>·3H<sub>2</sub>O (128 mg, 530 μmol) was added to a solution of 7 (300 mg, 354 μmol) in Ac<sub>2</sub>O (10 mL), and the reaction solution was stirred at room temperature for 24 h. After 20 mL of water was added, the resulting solution was extracted with CHCl<sub>3</sub> (30 mL × 3). The combined organic layer was dried over Na<sub>2</sub>SO<sub>4</sub>, filtered, and concentrated under reduced pressure, and the resulting residue was purified by silica gel column chromatography (hexanes/CHCl<sub>3</sub> = 3:2) and recrystallization from hexanes/CH<sub>2</sub>Cl<sub>2</sub> to afford 9 as an orange powder (336 mg, 96% yield). mp > 300 °C. IR (ATR): ν = 2925, 2854, 1590, 1539, 1493, 1319, 1294, 1256, 921, 823, 758 cm<sup>-1</sup>. <sup>1</sup>H NMR (300 MHz,

CDCl<sub>3</sub>/TMS): δ = 9.03 (s, 3H), 8.95 (d, J = 8.4 Hz, 3H), 7.86–7.75 (m, 9H), 7.36 (d, J = 6.2 Hz, 3H), 7.31 (d, J = 6.2 Hz, 3H), 6.87 (s, 3H), 2.45 (s, 9H) ppm. ESI-MS (*m/z*): Calcd for C<sub>48</sub>H<sub>33</sub>(<sup>191</sup>Ir)N<sub>6</sub> (M<sup>+</sup>): 980.2062. Found: 980.2061. Anal. Calcd for C<sub>48</sub>H<sub>33</sub>IrN<sub>6</sub>O<sub>6</sub>: C, 58.71; H, 3.39; N, 8.56. Found: C, 58.77; H, 3.16; N, 8.47%.

**fac-Tris[1-(5'-nitro-4'-trifluoromethylphenyl)isoquinoline]iridium(III) (Ir(tfpiq-NO<sub>2</sub>)<sub>3</sub>) (10).** Cu(NO<sub>3</sub>)<sub>2</sub>·3H<sub>2</sub>O (243 mg, 241 μmol) was added to a solution of 8 (174 mg, 723 μmol) in Ac<sub>2</sub>O (10 mL), and the reaction solution was stirred at room temperature for 24 h, after which 20 mL of water was added; the solution was then extracted with CHCl<sub>3</sub> (30 mL × 3). The combined organic layer was dried over Na<sub>2</sub>SO<sub>4</sub>, filtered, and concentrated under reduced pressure, and the resulting residue was purified by silica gel column chromatography (hexanes/CHCl<sub>3</sub> = 3:2) and recrystallization from hexanes/CH<sub>2</sub>Cl<sub>2</sub> to afford 10 as an orange powder (250 mg, 91% yield). mp > 300 °C. IR (ATR): ν = 1592, 1521, 1460, 1336, 1283, 1144, 1060, 1006, 908, 821, 732, 688, 647, 593 cm<sup>-1</sup>. <sup>1</sup>H NMR (300 MHz, CDCl<sub>3</sub>/TMS): δ = 8.86 (d, J = 6.1 Hz, 6H), 7.99–7.79 (m, 9H), 7.48 (d, J = 6.2 Hz, 3H), 7.40 (d, J = 6.2 Hz, 3H), 7.26 (s, 3H) ppm. ESI-MS (*m/z*): Calcd for C<sub>48</sub>H<sub>24</sub>F<sub>9</sub>(<sup>191</sup>Ir)N<sub>6</sub>O<sub>6</sub> (M<sup>+</sup>): 1142.1214. Found: 1142.1203. Anal. Calcd for C<sub>48</sub>H<sub>24</sub>F<sub>9</sub>IrN<sub>6</sub>O<sub>6</sub>·H<sub>2</sub>O: C, 49.62; H, 2.26; N, 7.23. Found: C, 49.81; H, 2.00; N, 7.25%.

**fac-Tris[1-(5'-amino-4'-methylphenyl)isoquinoline]iridium(III) (Ir(ampiq)<sub>3</sub>) (11).** SnCl<sub>2</sub>·2H<sub>2</sub>O (293 mg, 1.30 mmol) and NaBH<sub>4</sub> (49.2 mg, 1.30 mmol) were added to a solution of 9 (82.7 mg, 84.2 μmol) in EtOH (3 mL), and the reaction mixture was heated at reflux for 20 min. NaBH<sub>4</sub> (49.2 mg, 1.30 mmol) was added, and the reaction mixture was refluxed for 20 min. After the mixture cooled to room temperature, the insoluble materials were removed by filtration. After 15 mL of H<sub>2</sub>O was added to the filtrate, the solution was extracted with CHCl<sub>3</sub> (20 mL × 3). The combined organic layer was dried over Na<sub>2</sub>SO<sub>4</sub>, filtered, and concentrated under reduced pressure, and the resulting residue was purified by silica gel column chromatography (CHCl<sub>3</sub>/MeOH = 30:1 to 10:1) and recrystallization from hexanes/CH<sub>2</sub>Cl<sub>2</sub> to afford 11 (24.8 mg, 33% yield) as a dark red-brown powder. mp > 300 °C. IR (ATR): ν = 3341, 2923, 2853, 1615, 1591, 1535, 1500, 1438, 1402, 1347, 1297, 1266, 1122, 810, 750, 735, 639, 558, 418 cm<sup>-1</sup>. <sup>1</sup>H NMR (300 MHz, CDCl<sub>3</sub>/TMS): δ = 8.92 (m, 3H), 7.64–7.57 (m, 12H), 7.26 (m, 3H), 6.97 (d, J = 6.2 Hz, 3H), 6.71 (s, 3H), 2.02 (s, 9H) ppm. ESI-MS (*m/z*): Calcd for C<sub>48</sub>H<sub>39</sub>(<sup>191</sup>Ir)N<sub>6</sub> (M<sup>+</sup>): 890.2837. Found: 890.2835. Anal. Calcd for C<sub>48</sub>H<sub>39</sub>IrN<sub>6</sub>·0.5CH<sub>2</sub>Cl<sub>2</sub>·H<sub>2</sub>O: C, 61.15; H, 4.44; N, 8.82. Found: C, 61.46; H, 4.22; N, 8.80%.

**fac-Tris[1-(5'-amino-4'-trifluoromethylphenyl)isoquinoline]iridium(III) (Ir(atfpiq)<sub>3</sub>) (12).** SnCl<sub>2</sub>·2H<sub>2</sub>O (91.4 mg, 405 μmol) and NaBH<sub>4</sub> (15.5 mg, 410 μmol) were added to a solution of 10 (32.0 mg, 280 μmol) in EtOH (4 mL), and the reaction mixture was heated at reflux for 20 min. NaBH<sub>4</sub> (15.5 mg, 410 μmol) was added, and the reaction mixture was then refluxed for 20 min. After the mixture cooled to room temperature, the insoluble materials were removed by filtration. After adding 15 mL of H<sub>2</sub>O to the filtrate, the solution was extracted with CHCl<sub>3</sub> (20 mL × 3). The combined organic layer was dried over Na<sub>2</sub>SO<sub>4</sub>, filtered, and concentrated under reduced pressure, and the resulting residue was purified by silica gel column chromatography (CHCl<sub>3</sub>/MeOH = 50:1 to 10:1) and recrystallization from hexanes/CH<sub>2</sub>Cl<sub>2</sub> to afford 12 (11.4 mg, 39% yield) as a dark red-brown powder. mp > 300 °C. IR (ATR): ν = 3376, 1621, 1540, 1408, 1255, 1138, 1096, 1052, 1019, 896, 817, 743, 701, 546 cm<sup>-1</sup>. <sup>1</sup>H NMR (300 MHz, CDCl<sub>3</sub>/TMS): δ = 8.94–8.83 (m, 3H), 7.78–7.74 (m, 3H), 7.71–7.67 (m, 9H), 7.30 (d, J = 6.3 Hz, 3H), 6.93 (d, J = 6.3 Hz, 3H), 6.95 (s, 3H) ppm. ESI-MS (*m/z*): Calcd for C<sub>48</sub>H<sub>30</sub>F<sub>9</sub>(<sup>191</sup>Ir)N<sub>6</sub> (M<sup>+</sup>): 1052.1989. Found: 1052.1987. Anal. Calcd for C<sub>48</sub>H<sub>30</sub>F<sub>9</sub>IrN<sub>6</sub>·1/4H<sub>2</sub>O: C, 54.47; H, 2.90; N, 7.94. Found: C, 54.86; H, 2.75; N, 7.54%.

**fac-Tris[1-(5'-diethylamino-4'-methylphenyl)isoquinoline]iridium(III) (Ir(deampiq)<sub>3</sub>) (13).** Ethyl iodide (1.90 g, 12.2 mmol) and Cs<sub>2</sub>CO<sub>3</sub> (397 mg, 1.22 mmol) were added to a solution of 11 (30.2 mg, 33.9 μmol) in MeCN (2.0 mL). The reaction mixture was stirred at room temperature for 12 h, and the insoluble materials were removed by filtration. The filtrate was washed with CHCl<sub>3</sub>, concentrated under the reduced pressure, and diluted with CHCl<sub>3</sub>. The resulting CHCl<sub>3</sub> solution was washed with 1N NaOH (aq), and the combined organic

layer was dried over  $\text{Na}_2\text{SO}_4$ , filtered, and concentrated under reduced pressure. The resulting residue was purified by NH silica gel column chromatography (hexanes/ $\text{CHCl}_3 = 2:1$ ), and the eluted solution containing **13** was combined, washed with 1N NaOH (aq), and concentrated (this manipulation is necessary to obtain clear  $^1\text{H}$  NMR spectra). The resulting material was recrystallization from hexanes/ $\text{CH}_2\text{Cl}_2$  to afford **13** as a dark red-brown powder (19.0 mg, 53% from **11**). mp > 300 °C. IR (ATR):  $\nu = 2966, 2803, 1581, 1498, 1437, 1378, 1343, 1258, 1107, 1084, 812, 739, 637, 565, 415 \text{ cm}^{-1}$ .  $^1\text{H}$  NMR (300 MHz,  $\text{CDCl}_3/\text{TMS}$ ):  $\delta = 8.84\text{--}8.74$  (m, 3H), 7.86 (s, 3H), 7.72–7.68 (m, 3H), 7.64–7.60 (m, 6H), 7.17 (d,  $J = 6.2 \text{ Hz}$ , 3H), 7.03 (d,  $J = 6.2 \text{ Hz}$ , 3H), 6.65 (s, 3H), 3.14–2.88 (m, 12H), 2.11 (s, 9H), 1.00 (t,  $J = 7.0 \text{ Hz}$ , 18H) ppm. ESI-MS ( $m/z$ ): Calcd for  $\text{C}_{60}\text{H}_{64}(\text{Ir})\text{N}_6$  ( $\text{M}+\text{H}$ ) $^+$ : 1059.4793. Found: 1059.4794. Anal. Calcd for  $\text{C}_{60}\text{H}_{63}\text{IrN}_6\cdot\text{H}_2\text{O}$ : C, 66.82; H, 6.08; N, 7.79. Found: C, 66.76; H, 5.85; N, 7.83%.

**fac-Tris[1-(5'-bis-Cbz-guanidyl-4'-methylphenyl)isoquinoline]iridium(III) (Ir(Cbz-gmpiq) $_3$ ) (21) (Cbz = carbobenzoxy).** The synthesis of this compound was performed using the method reported for the guanidyl compounds.<sup>16</sup> Triethylamine (27.2 mg, 269  $\mu\text{mol}$ ) and  $\text{HgCl}_2$  (20.0 mg, 73.7  $\mu\text{mol}$ ) were added to a solution of **11** (20.0 mg, 22.4  $\mu\text{mol}$ ) and **19**<sup>17</sup> (25.3 mg, 70.6  $\mu\text{mol}$ ) in dry dimethylformamide (DMF, 2.0 mL) at 0 °C. The resulting brown suspension was stirred at 0 °C for 1 h, and the mixture was diluted with  $\text{CHCl}_3$  and filtered. The filtrate was washed with water (30 mL) and dissolved in  $\text{CHCl}_3$  (30 mL  $\times$  3). The organic layer was washed with water, dried over  $\text{Na}_2\text{SO}_4$ , and filtered. Evaporation of the solvent gave a crude product that was purified by silica gel column chromatography ( $\text{CHCl}_3$ ) followed by GPC ( $\text{CHCl}_3$ ). The resulting material was recrystallized from hexanes/ $\text{CH}_2\text{Cl}_2$  to afford **21** as a red-brown powder (29.5 mg, 72% from **11**). mp > 300 °C. IR (ATR):  $\nu = 1725, 1615, 1546, 1498, 1421, 1398, 1363, 1325, 1234, 1206, 1119, 1051, 908, 803, 734, 694, 633, 581, 558, 384 \text{ cm}^{-1}$ .  $^1\text{H}$  NMR (300 MHz,  $\text{CDCl}_3/\text{TMS}$ ):  $\delta = 12.04$  (s, 3H), 10.12 (s, 3H), 9.17 (d,  $J = 8.7 \text{ Hz}$ , 3H), 8.57 (s, 3H), 7.59 (d,  $J = 8.4 \text{ Hz}$ , 3H), 7.43–7.29 (m, 21H), 7.26 (s, 6H), 7.20 (d,  $J = 6.3 \text{ Hz}$ , 3H), 7.06 (t,  $J = 7.5 \text{ Hz}$ , 3H), 6.99 (d,  $J = 6.3 \text{ Hz}$ , 3H), 6.82 (s, 3H), 5.20 (d,  $J = 8.7 \text{ Hz}$ , 12H), 2.13 (s, 9H) ppm. ESI-MS ( $m/z$ ): Calcd for  $\text{C}_{99}\text{H}_{82}(\text{Ir})\text{N}_{12}\text{O}_{12}$  ( $\text{M}+\text{H}$ ) $^+$ : 1821.5776. Found: 1821.5764. Anal. Calcd for  $\text{C}_{99}\text{H}_{81}\text{IrN}_{12}\text{O}_{12}\cdot 1.5\text{H}_2\text{O}$ : C, 64.27; H, 4.58; N, 9.09. Found: C, 64.19; H, 4.22; N, 9.09%.

**fac-Tris[1-(5'-guanidyl-4'-methylphenyl)isoquinoline]iridium(III) (Ir(gmpiq) $_3$ ) (14).** Compound **21** (29.1 mg, 15.9  $\mu\text{mol}$ ) was dissolved in tetrahydrofuran (THF)/MeOH (4/1 v/v, 10 mL), and 20 mg of 10% Pd/C was added. The hydrogenation reaction was performed at room temperature under  $\text{H}_2$  atmosphere for 8 h. The catalyst was removed by filtration through a pad of diatomaceous earth, and the filtrate was concentrated under reduced pressure. The resulting residue was purified by  $\text{Al}_2\text{O}_3$  column chromatography ( $\text{CH}_2\text{Cl}_2$  to MeOH) and recrystallization from Et $_2\text{O}/\text{CH}_2\text{Cl}_2/\text{MeOH}$  to afford **14** as a red-brown powder (14.0 mg, 86% from **21**). mp > 300 °C. IR (ATR):  $\nu = 3147, 1614, 1436, 1396, 1260, 1037, 879, 837, 816, 740, 633 \text{ cm}^{-1}$ .  $^1\text{H}$  NMR (300 MHz,  $\text{CD}_3\text{OD}/\text{TMS}$ ):  $\delta = 8.82\text{--}8.79$  (m, 3H), 7.89 (s, 3H), 7.80–7.76 (m, 3H), 7.67–7.64 (m, 6H), 7.26–7.21 (m, 6H), 6.82 (s, 3H), 1.96 (s, 9H) ppm. ESI-MS ( $m/z$ ): Calcd for  $\text{C}_{51}\text{H}_{45}(\text{Ir})\text{N}_{12}$  ( $\text{M}^+$ ): 1016.3491. Found: 1016.3491. Anal. Calcd for  $\text{C}_{51}\text{H}_{45}\text{IrN}_{12}\cdot 5.5\text{SCH}_2\text{Cl}_2\cdot\text{Et}_2\text{O}$ : C, 46.60; H, 4.27; N, 10.78. Found: C, 46.74; H, 4.26; N, 10.99%.

**1,3-Bis(Cbz)imidazolidine-2-thione (20).** Compound **20** was synthesized according to a reported method for the Cbz protection of some amines.<sup>18</sup> A mixture of imidazolidine-2-thione (1.00 g, 9.79 mmol) and NaH (55%, 1.28 g, 29.4 mmol) in 20 mL of dry THF was stirred at room temperature for 2 h. Benzyl chloroformate (502 mg, 29.4 mmol) was then added dropwise at 0 °C, and the resulting mixture was stirred at room temperature for 3 h and quenched by adding water to the reaction mixture. The reaction mixture was extracted with AcOEt, and the combined organic layer was washed with water twice, once with brine, dried over  $\text{Na}_2\text{SO}_4$ , and filtered. Evaporation of the solvent gave a crude product that was purified by silica gel column chromatography ( $\text{CHCl}_3$ ) and concentrated. The resulting material was recrystallized from hexanes/ $\text{CH}_2\text{Cl}_2$  to afford **20** as a pale yellow crystal (2.17 g, 5.85 mmol, 60% from imidazolidine-2-thione). mp > 300 °C. IR (ATR):  $\nu = 1756, 1455, 1379, 1251, 1251, 1207, 1141, 987, 919, 751, 691, 608, 473 \text{ cm}^{-1}$ .  $^1\text{H}$  NMR (300 MHz,  $\text{CDCl}_3/\text{TMS}$ ):  $\delta = 7.44\text{--}7.34$  (m, 10H), 5.30 (s, 4H), 4.00

(s, 4H) ppm. ESI-MS ( $m/z$ ): Calcd for  $\text{C}_{19}\text{H}_{19}\text{N}_2\text{O}_4\text{S}$  ( $\text{M}+\text{H}$ ) $^+$ : 371.1060. Found: 371.1069. Anal. Calcd for  $\text{C}_{19}\text{H}_{18}\text{N}_2\text{O}_4\text{S}$ : C, 61.61; H, 4.90; N, 7.56. Found: C, 61.79; H, 4.75; N, 7.70%.

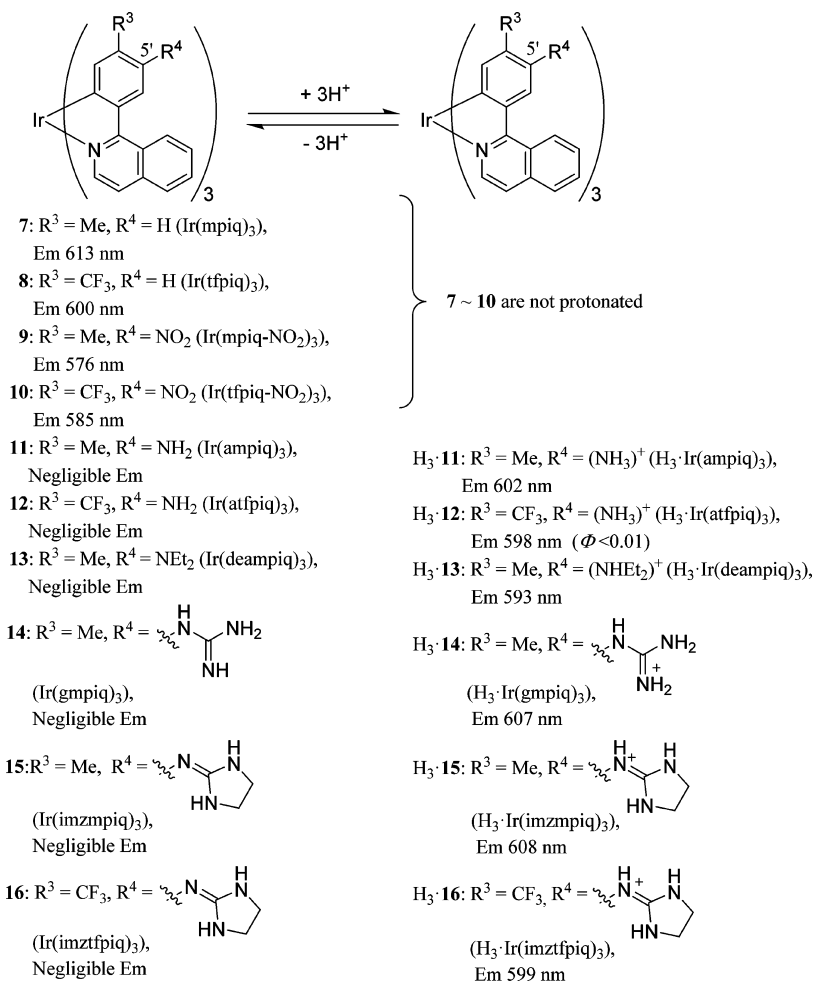
**fac-Tris[1-(5'-bis-Cbz-iminoimidazolidinyl-4'-methylphenyl)isoquinoline]iridium(III) (Ir(Cbz-imzmpiq) $_3$ ) (22).** The synthesis of this compound was performed using the method reported for the iminoimidazolidinyl compounds.<sup>19</sup> Triethylamine (42.9 mg, 425  $\mu\text{mol}$ ) and  $\text{HgCl}_2$  (28.8 mg, 106  $\mu\text{mol}$ ) was added to solution of **11** (31.6 mg, 35.4  $\mu\text{mol}$ ) and **20** (41.3 mg, 112  $\mu\text{mol}$ ) in dry DMF (2.0 mL) at 0 °C. The resulting brown suspension was stirred at 0 °C for 1.5 h, and the mixture was diluted with  $\text{CHCl}_3$  and filtered. The filtrate was washed with water (30 mL) and extracted with  $\text{CHCl}_3$  (30 mL  $\times$  3). The organic layer was washed with water, dried over  $\text{Na}_2\text{SO}_4$ , and filtered. Evaporation of the filtrate gave a crude product that was purified by silica gel column chromatography ( $\text{CHCl}_3$ ) followed by GPC ( $\text{CHCl}_3$ ) and concentrated. The resulting material was recrystallized from hexanes/ $\text{CH}_2\text{Cl}_2$  to afford **22** as a red-brown powder (36.2 mg, 53% from **11**). mp > 300 °C. IR (ATR):  $\nu = 1760, 1698, 1499, 1454, 1382, 1295, 1207, 1146, 1106, 999, 813, 755, 737, 697, 400 \text{ cm}^{-1}$ .  $^1\text{H}$  NMR (300 MHz,  $\text{CDCl}_3/\text{TMS}$ ):  $\delta = 8.66$  (d,  $J = 8.1 \text{ Hz}$ , 3H), 7.55–7.51 (m, 6H), 7.45 (d,  $J = 7.2 \text{ Hz}$ , 3H), 7.26–7.11 (m, 51H), 6.98 (d,  $J = 6.3 \text{ Hz}$ , 3H), 3.92–3.81 (m, 6H), 3.78–3.68 (m, 6H), 1.89 (s, 9H) ppm. ESI-MS ( $m/z$ ): Calcd for  $\text{C}_{105}\text{H}_{88}(\text{Ir})\text{N}_{12}\text{O}_{12}$  ( $\text{M}+\text{H}$ ) $^+$ : 1899.6245. Found: 1899.6252. Anal. Calcd for  $\text{C}_{105}\text{H}_{87}\text{IrN}_{12}\text{O}_{12}\cdot 2\text{H}_2\text{O}$ : C, 65.10; H, 4.74; N, 8.84. Found: C, 64.92; H, 4.35; N, 8.58%.

**fac-Tris[1-(5'-iminoimidazolidinyl-4'-methylphenyl)isoquinoline]iridium(III) (Ir(imzmpiq) $_3$ ) (15).** Compound **22** (17 mg, 8.9  $\mu\text{mol}$ ) was dissolved in THF/MeOH (1/1 v/v, 4 mL), and 13 mg of 10% Pd/C was added. The hydrogenation reaction was performed at room temperature under  $\text{H}_2$  atmosphere for 3 h. The catalyst was removed by filtration through a pad of diatomaceous earth, and the filtrate was concentrated under reduced pressure. The resulting residue was purified by  $\text{Al}_2\text{O}_3$  column chromatography ( $\text{CH}_2\text{Cl}_2/\text{MeOH}$ ) and recrystallization from  $\text{CH}_2\text{Cl}_2/\text{MeOH}$  to afford **15** as a red-brown powder (8.0 mg, 82% from **22**). mp > 300 °C. IR (ATR):  $\nu = 2919, 2851, 1652, 1586, 1542, 1499, 1436, 1395, 1346, 1260, 1085, 1031, 814, 736, 559 \text{ cm}^{-1}$ .  $^1\text{H}$  NMR (300 MHz,  $\text{CD}_3\text{OD}/\text{TMS}$ ):  $\delta = 8.91\text{--}8.88$  (m, 3H), 8.07 (s, 3H), 7.92–7.89 (m, 3H), 7.79–7.76 (m, 6H), 7.36 (s, 6H), 6.92 (s, 3H), 3.72 (s, 12H), 2.07 (s, 9H) ppm. ESI-MS ( $m/z$ ): Calcd for  $\text{C}_{57}\text{H}_{52}(\text{Ir})\text{N}_{12}$  ( $\text{M}+\text{H}$ ) $^+$ : 1095.4038. Found: 1095.4027. Anal. Calcd for  $\text{C}_{57}\text{H}_{51}\text{IrN}_{12}\cdot 3\text{CH}_2\text{Cl}_2\cdot\text{H}_2\text{O}$ : C, 52.64; H, 4.34; N, 12.28. Found: C, 52.93; H, 4.40; N, 12.58%.

**fac-Tris[1-(5'-bis-Cbz-iminoimidazolidinyl-4'-trifluoromethylphenyl)isoquinoline]iridium(III) (Ir(Cbz-imztfpiq) $_3$ ) (23).** Triethylamine (55.2 mg, 546  $\mu\text{mol}$ ) and  $\text{HgCl}_2$  (37.4 mg, 138  $\mu\text{mol}$ ) were added to a solution of **12** (48.0 mg, 45.5  $\mu\text{mol}$ ) and **20** (53.2 mg, 144  $\mu\text{mol}$ ) in dry DMF (4.0 mL) at 0 °C. The reaction mixture was stirred at 0 °C for 2 h, diluted with  $\text{CHCl}_3$ , and filtered. The filtrate was washed with water (30 mL) and extracted with  $\text{CHCl}_3$  (30 mL  $\times$  3). The combined organic layer was washed with water, dried over  $\text{Na}_2\text{SO}_4$ , filtered, and concentrated under reduced pressure. The resulting crude product was purified by silica gel column chromatography (hexanes/ $\text{CHCl}_3$ ) followed by GPC ( $\text{CHCl}_3$ ) and concentrated. The resulting material was recrystallized from hexanes/ $\text{CH}_2\text{Cl}_2$  to afford **23** as a red-brown powder (49.0 mg, 52% from **12**). mp > 300 °C. IR (ATR):  $\nu = 1763, 1693, 1379, 1290, 1208, 1140, 1116, 1056, 998, 905, 819, 730, 697 \text{ cm}^{-1}$ .  $^1\text{H}$  NMR (300 MHz,  $\text{CDCl}_3/\text{TMS}$ ):  $\delta = 8.69\text{--}8.66$  (m, 3H), 7.68 (d,  $J = 6.3 \text{ Hz}$ , 3H), 7.62 (s, 3H), 7.57–7.54 (m, 3H), 7.45 (s, 3H), 7.38–7.35 (m, 6H), 7.24–7.17 (m, 33H), 7.10–7.02 (m, 12H), 3.85–3.76 (m, 12H) ppm. ESI-MS ( $m/z$ ): Calcd for  $\text{C}_{105}\text{H}_{79}\text{F}_9(\text{Ir})\text{N}_{12}\text{O}_{12}$  ( $\text{M}+\text{H}$ ) $^+$ : 2061.5397. Found: 2061.5429. Anal. Calcd for  $\text{C}_{105}\text{H}_{78}\text{F}_9\text{IrN}_{12}\text{O}_{12}\cdot\text{H}_2\text{O}$ : C, 60.60; H, 3.87; N, 8.08. Found: C, 60.35; H, 3.47; N, 8.11%.

**fac-Tris[1-(5'-iminoimidazolidinyl-4'-trifluoromethylphenyl)isoquinoline]iridium(III) (Ir(imztfpiq) $_3$ ) (16).** Compound **23** (34.9 mg, 16.9  $\mu\text{mol}$ ) was dissolved in THF/MeOH (1/1 v/v, 5 mL), and 25 mg of 10% Pd/C was added. The hydrogenation reaction was performed in a Parr hydrogenation apparatus for 6 h. The catalyst was removed by filtration through a pad of diatomaceous earth, and the filtrate was concentrated under reduced pressure. The resulting residue was purified by  $\text{Al}_2\text{O}_3$  column chromatography ( $\text{CH}_2\text{Cl}_2/\text{MeOH}$ ) and recrystallization from  $\text{CH}_2\text{Cl}_2/\text{MeOH}$  to afford **16** as a red-brown

Chart 2



powder (19.4 mg, 91% from 23). mp > 300 °C. IR (ATR):  $\nu = 2877, 1655, 1589, 1392, 1305, 1244, 1217, 1112, 1055, 901, 817, 749, 712, 670 \text{ cm}^{-1}$ .  $^1\text{H}$  NMR (300 MHz,  $\text{CD}_3\text{OD}/\text{TMS}$ ):  $\delta = 8.93\text{--}8.89$  (m, 3H), 8.02 (s, 3H), 7.95–7.90 (m, 3H), 7.82–7.78 (m, 6H), 7.45 (d,  $J = 6.0 \text{ Hz}$ , 3H), 7.34 (d,  $J = 6.0 \text{ Hz}$ , 3H), 7.17 (s, 3H), 3.54 (s, 12H) ppm. ESI-MS ( $m/z$ ): Calcd for  $\text{C}_{57}\text{H}_{42}\text{F}_9(^{191}\text{Ir})\text{N}_{12}$  ( $\text{M}+\text{H}^+$ ): 1257.3190. Found: 1257.3117. Anal. Calcd for  $\text{C}_{57}\text{H}_{42}\text{F}_9\text{IrN}_{12} \cdot \text{CH}_2\text{Cl}_2 \cdot \text{MeOH}$ : C, 51.53; H, 3.52; N, 12.22. Found: C, 51.73; H, 3.22; N, 12.00%.

**Crystallographic Study of 9 ( $\text{Ir}(\text{mpiq-NO}_2)_3$ ).** A red block crystal of 9 was obtained from the slow diffusion of  $\text{Et}_2\text{O}$  into a  $\text{CH}_2\text{Cl}_2$  solution of 9. All measurements were performed using a Bruker APEX CCD area detector using Mo  $K\alpha$  radiation at  $-170^\circ\text{C}$ . The structure was solved by direct methods. All calculations were performed using the Crystal Structure crystallographic software package except for refinements, which were performed using SHELXL-97. Crystal data:  $\text{C}_{48}\text{H}_{33}\text{IrN}_6\text{O}_6$ ,  $M_r = 982.00$ , monoclinic, space group  $C/2c$ ,  $T = 273 \text{ K}$ ,  $a = 19.902(3)$ ,  $b = 29.796(4)$ ,  $c = 17.541(2) \text{ \AA}$ ,  $\alpha = 90^\circ$ ,  $\beta = 95.096(2)^\circ$ ,  $\gamma = 90^\circ$ ,  $V = 10360(2) \text{ \AA}^3$ ,  $Z = 8$ ,  $\rho_{\text{calcd}} = 1.259 \text{ g}\cdot\text{cm}^{-3}$ ,  $2\theta_{\text{max}} = 24.94^\circ$ ,  $R = 0.0573$  (for 7237 reflections with  $I > 2\sigma(I)$ ),  $R_w = 0.1935$  (for 9017 reflections),  $\text{GOF} = 1.076$ . Additional crystallographic information is available in the Supporting Information.

**Measurements of UV–vis Absorption and Luminescence Spectra.** UV–vis spectra were recorded on a Jasco V-550 UV–vis spectrophotometer and emission spectra were recorded on a Jasco FP-6200 spectrofluorometer at  $25^\circ\text{C}$ . Sample solutions in quartz cuvettes equipped with Teflon septum screw caps were degassed by bubbling Ar through the solution for 10 min prior to making the luminescence measurements. The quantum yields for luminescence ( $\Phi$ ) were determined by comparison with the integrated corrected emission spectrum of a quinine sulfate standard, whose emission quantum yield in 0.1 M

$\text{H}_2\text{SO}_4$  was assumed to be 0.55 (excitation at 366 nm) and corrected by using the standard  $\Phi$  value of  $\text{Ir}(\text{mpiq})_3$  (7) ( $\Phi = 0.26$ ).<sup>13</sup> eq 1 was used to calculate the emission quantum yields, in which  $\Phi_s$  and  $\Phi_r$  denote the quantum yields of the sample and reference compound;  $\eta_s$  and  $\eta_r$  are the refractive indexes of the solvents used for the measurements of the sample and the reference (1.477 for dimethyl sulfoxide (DMSO) ( $\eta_s$ ) and 1.333 for  $\text{H}_2\text{O}$  ( $\eta_r$ ));  $A_s$  and  $A_r$  are the absorbance of the sample and the reference; and  $I_s$  and  $I_r$  stand for the integrated areas under the emission spectra of the sample and reference, respectively (all of the Ir compounds were excited at 366 nm for luminescence measurements in this study). For the determination of  $\Phi_s$  in mixed-solvent systems, the  $\eta$  values of the main solvents were used for the calculation.

$$\Phi_s = \Phi_r(\eta_s^2 A_r I_s) / (\eta_r^2 A_s I_r) \quad (1)$$

The luminescence lifetimes of sample solutions in degassed DMSO at  $25^\circ\text{C}$  were measured on a TSP1000-M-PL (Unisoku, Osaka, Japan) instrument by using third harmonic generation (THG) (355 nm) of Nd:YAG laser, Minilite I (Continuum, CA) as excitation source. The signals were monitored with an R2949 photomultiplier. Data were analyzed by using the nonlinear least-squares procedure.

**Cell Culturing and Luminescence Imaging.** HeLa-S3 cells, provided by Dr. Tomoko Okada (National Institute of Advanced Industrial Science and Technology), were grown in MEM supplemented with 10% fetal calf serum (FCS) under 5%  $\text{CO}_2$  at  $37^\circ\text{C}$ . HeLa-S3 cells ( $2.0 \times 10^5$  cells/mL) were plated in 1.0 mL of MEM on  $35 \times 10 \text{ mm}$  Greiner CELLview Petri Dish, Four Compartments (Greiner) under the same conditions and allowed to adhere for 24 h. Subsequently, 0.5 mL of MEM containing Ir complexes (50  $\mu\text{M}$ ) in MEM/DMSO (9S/5, v/v) was added, and the samples in MEM/DMSO (9S/5, v/v) were incubated at  $37^\circ\text{C}$  under 5%  $\text{CO}_2$  for 30 min. The culture medium was then removed

Table 1

17 (mpiq): R<sup>3</sup> = Me  
18 (tfpiq): R<sup>3</sup> = CF<sub>3</sub>

7 (*fac*-Ir(mpiq)<sub>3</sub>): R<sup>3</sup> = Me  
8 (*fac*-Ir(tfpiq)<sub>3</sub>): R<sup>3</sup> = CF<sub>3</sub>

| entry | ligand                           | conditions               | yield                                   |
|-------|----------------------------------|--------------------------|---|
| 1     | R <sup>3</sup> = Me              | reflux, 7 d              | <i>fac</i> -7: 67% <i>mer</i> -7: trace |
| 2     | R <sup>3</sup> = Me              | microwave, 50 min, twice | <i>fac</i> -7: 50% <i>mer</i> -7: trace |
| 3     | R <sup>3</sup> = CF <sub>3</sub> | reflux, 7 d              | <i>fac</i> -8: 3% <i>mer</i> -8: 35%    |
| 4     | R <sup>3</sup> = CF <sub>3</sub> | microwave, 50 min, twice | <i>fac</i> -8: 60% <i>mer</i> -8: trace |

and washed twice with phosphate buffered saline (PBS). Finally, 0.5 mL of MEM was added for luminescence imaging by confocal microscopy (Leica TCS SP2, Leica) with an excitation wavelength at 350, 360, and 458 nm for Ir complexes and 488 nm for MitoTracker and LysoTracker. The emission of Ir complexes was measured at 580–650 nm, and that of MitoTracker and LysoTracker was measured at 490–550 nm using a prism spectrometer.

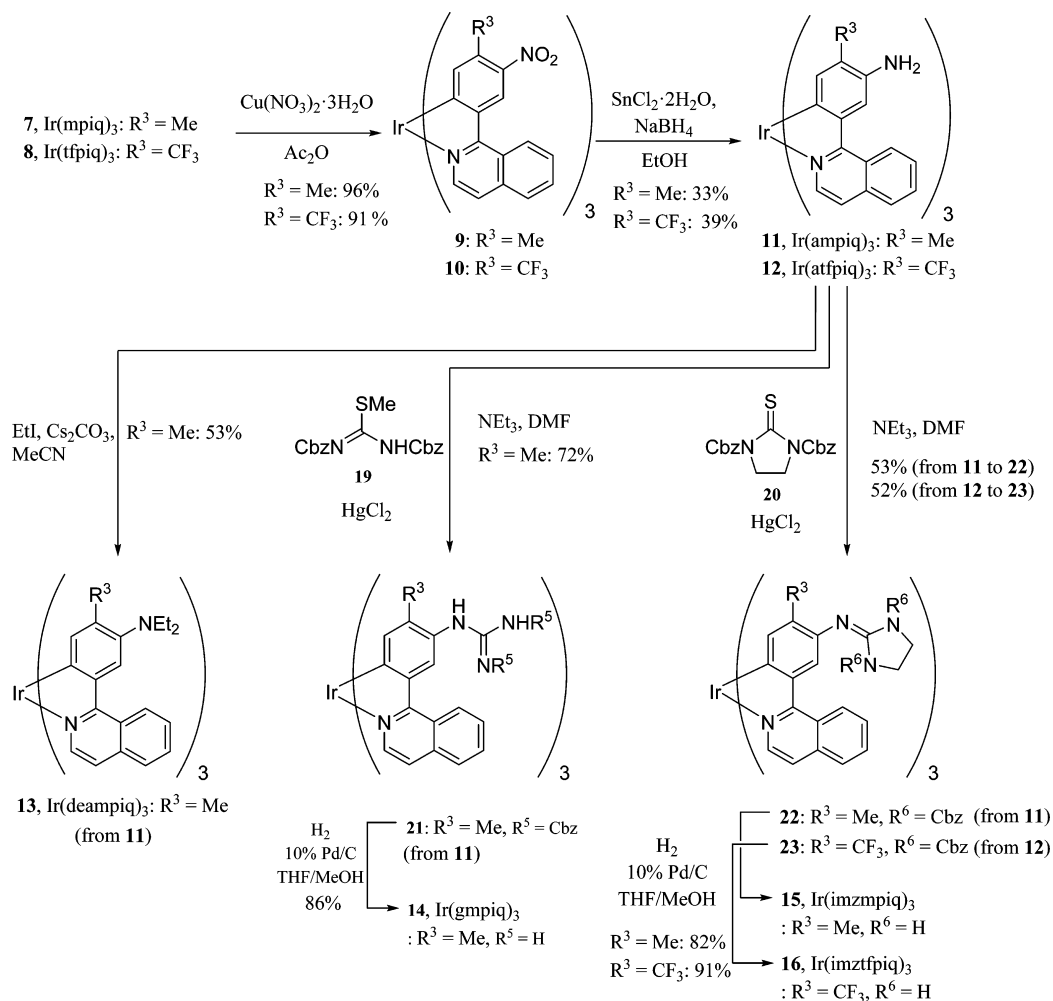
**Photoinduced Cell Death and Propidium Iodide Staining.** HeLa-S3 cells were incubated in MEM/DMSO (99/1, v/v) containing the Ir complex (10 μM) for 30 min at 37 °C, and washed twice with PBS.

A 100 μL aliquot of MEM was added, and the solution was then subjected to photoirradiation at 465 nm (Twinlight 465, RELYON, Japan; the number of photon per second was determined to be  $1.3 \times 10^{-4}$  mol/s by means of ferrioxalate actinometry)<sup>20</sup> at 25 °C. After photoirradiation, the solution was incubated for 2 h, and 3.0 μL of PI solution (1 mM) was then added, followed by incubation for 30 min at 37 °C. The culture medium was then removed and washed twice with PBS. Finally, 100 μL of MEM was added for observation (excitation at 540 nm for PI) on a BIOREVO BZ-9000 instrument (Keyence, Japan).

**Singlet Oxygen Trapping Experiments in DMSO/H<sub>2</sub>O (3/2).**<sup>11c,d</sup> The solutions of Ir complexes (12 μM) in DMSO/H<sub>2</sub>O (1.3/1.2 v/v, 2.5 mL) were bubbled with O<sub>2</sub> for 10 min, to which a solution of DPBF (300 μM) in DMSO (500 μL) was added. The protonated Ir complexes (10 μM) were prepared in situ upon the addition of 0.01 M HCl aq (final concentration: 50 μM HCl). Measurement of <sup>1</sup>O<sub>2</sub> generation by deprotonated and protonated forms of Ir complexes was performed separately. The resulting solutions containing Ir complex (10 μM) and DPBF (50 μM) in DMSO/H<sub>2</sub>O (3/2) were photoirradiated at 470 nm (FP-6200, Jasco; the number of photon per second was determined to be  $9.7 \times 10^{-7}$  mol/s by means of ferrioxalate actinometry)<sup>20</sup> at 25 °C, and changes in the UV–vis spectra of DPBF were recorded.

**Electron Spin Resonance Analysis of Nitroxide Radical Generated by Reaction of TPC with Singlet Oxygen in DMSO/H<sub>2</sub>O (3/2).**<sup>11d</sup> Solutions of Ir complexes (40 μM) and 2,2,5,5-tetramethyl-3-pyrroline-3-carboxamide (TPC, 80 mM) in DMSO/H<sub>2</sub>O (3/2 v/v, 200 μL) were prepared, and then the solutions were photoirradiated at 465 nm (Twinlight 465, RELYON, Japan) at 25 °C. After the photoirradiation, the samples were transferred to a quartz cell, and electron spin resonance (ESR) spectra were recorded on an X-band ESR

Chart 3



spectrometer (JES-FA-100, JEOL, Tokyo, Japan). The measurement conditions for ESR were as follows: field sweep, 330.50–340.50 mT; field modulation frequency, 100 kHz; field modulation width, 0.05 mT; amplitude, 80; sweep time, 2 min; time constant, 0.03 s; microwave frequency, 9.420 GHz; microwave power, 4 mW. To calculate the spin concentration of each nitroxide radical, 20  $\mu\text{M}$  TEMPOL was used as a standard sample, and the ESR spectrum of manganese ( $\text{Mn}^{2+}$ ), which was located in the ESR cavity, was used as an internal standard. The spin concentration was determined using Digital Data Processing (JEOL, Tokyo, Japan).

## RESULTS AND DISCUSSION

**Synthesis of  $\text{Ir}(\text{mpiq})_3$  Derivatives.** Prior to the design of new Ir(III) complexes, we predicted the  $\text{p}K_a$  values of some derivatives of **7** based on the known aniline derivatives using the SciFinder database, as summarized in Figure S1 in Supporting Information. We previously reported that the introduction of  $N,N$ -diethylamino groups to the 5' position of  $\text{Ir}(\text{tpy})_3$  **2** to obtain  $\text{Ir}(\text{deatpy})_3$  **5**, which has  $\text{p}K_a$  value of ca. 7.<sup>11c</sup> Therefore, we introduced  $N,N$ -diethylamino groups on  $\text{Ir}(\text{mpiq})_3$  **7** and obtained **13** (Chart 2). Because the  $\text{p}K_a$  value of **13** was lower than predicted, as described below, we synthesized **14** and **15**, containing guanidyl and iminoimidazolidinyl groups, respectively. In addition, **16** was synthesized by introducing a trifluoromethyl group to permit the fine-tuning of the  $\text{p}K_a$  value based on the aforementioned prediction (Figure S1 in Supporting Information).

The *fac*- $\text{Ir}(\text{mpiq})_3$  **7** was prepared as a racemic mixture of  $\Delta$  and  $\Lambda$  forms in 67% yield from  $\text{IrCl}_3 \cdot 3\text{H}_2\text{O}$  and the *mpiq* ligand (30 equiv) in dioxane/ $\text{H}_2\text{O}$  under reflux for one week using our previously reported procedure (entry 1 in Table 1).<sup>11a</sup> When we applied this method to the preparation of **8**, the *facial* form of **8** (*fac*-**8**) was obtained in only 3% yield, and major product was the *meridional* form (*mer*-**8**, 35%, entry 3 in Table 1). Alternatively, microwave irradiation resulted in a considerable improvement in the chemical yield (60% in 100 min) of *fac*-**8** (entry 4 in Table 1), and **7** was obtained in moderate yield (50%) under the same conditions (entry 2 in Table 1). Note that a smaller amount of ligand (30 equiv against  $\text{IrCl}_3$ ) is required than that in the reported procedure.<sup>21</sup>

The nitration of **7** and **8** was then performed using  $\text{Cu}(\text{NO}_3)_2$  and  $\text{Ac}_2\text{O}$  to give the tris(nitro) derivatives **9** and **10**, and their nitro groups were then reduced with  $\text{SnCl}_2 \cdot 2\text{H}_2\text{O}$  and  $\text{NaBH}_4$  to give **11** and **12** (Chart 3).<sup>11a</sup> The tris(diethylamino) derivative  $\text{Ir}(\text{deampiq})_3$  **13** was obtained by the ethylation of **11**. The reaction of **11** with the Cbz-protected *S*-methylthiourea **19** gave **21**,<sup>16</sup> the Cbz groups of which were removed by hydrogenation to give  $\text{Ir}(\text{gmpiq})_3$  **14**. For the synthesis of  $\text{Ir}(\text{imzmpiq})_3$  **15**, we treated **11** with **20** to produce **22**, and its Cbz groups were deprotected. Similarly,  $\text{Ir}(\text{imztpiq})_3$  **16** was synthesized from **12** via **23**.

The structure of **9** was confirmed by a X-ray single-crystal structure analysis of fine red crystals obtained by recrystallization from  $\text{Et}_2\text{O}/\text{CH}_2\text{Cl}_2$ , as displayed in Figure 1a,b. Representative parameters for the crystal structure of **9** are listed in Table S1 in Supporting Information.<sup>22</sup>

**Photophysical Properties of **11**–**16**.** UV–vis spectra of the Ir(III) complexes **2** and **7**–**10** in DMSO at 25 °C are shown in Figure S3 in Supporting Information. Because of the extension of  $\pi$ -conjugation by the isoquinoline parts, the absorption spectra of **7**–**10** are red-shifted considerably, in comparison with that of  $\text{Ir}(\text{tpy})_3$  **2**, which contains phenylpyridine units. Their emission wavelength and luminescent quantum yields ( $\Phi$ ) (determined based on the standard complex  $\text{Ir}(\text{mpiq})_3$  **7** ( $\Phi = 0.26$  in toluene)<sup>13</sup>) are summarized in Table 2.

As shown in Figure 2a,b, the addition of  $\text{H}^+$  induced a considerable blue shift in the UV–vis absorption spectra of **11** (ca. 90 nm) and **16** (ca. 50 nm), and almost the same behaviors were observed for **12**–**15** (Figure S3 in Supporting Information). Figure 2c,e displays that acid-free **11** and **16** had a very weak emission and that the addition of HCl (in 1,4-dioxane) induced a considerable enhancement in their emission at

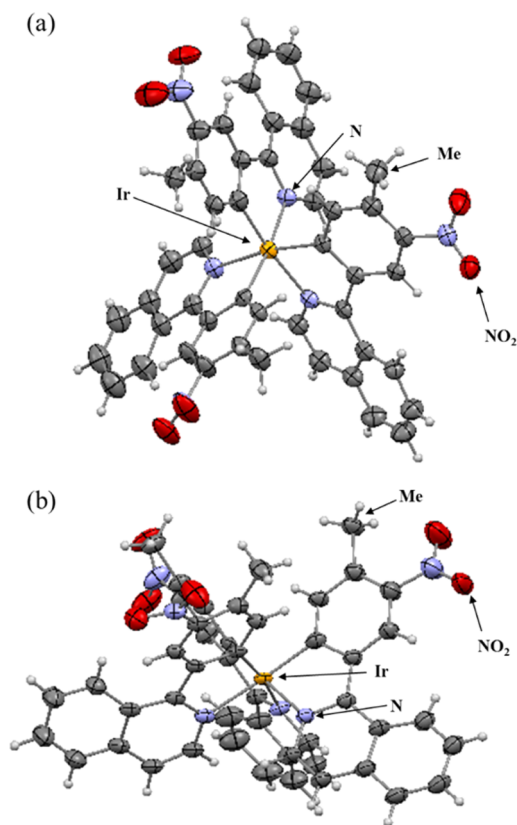


**Figure 1.** (a) Top and (b) side views of X-ray structure of **9** with thermal ellipsoids (50% probability).

**Table 2. Photophysical Properties of **7**–**16** (10  $\mu\text{M}$ ) in Degassed DMSO at 25 °C**

| complex               | $\lambda_{\text{max}}$ (absorption) | $\lambda_{\text{max}}^a$ (emission) | $\Phi^b$ | $\tau$ ( $\mu\text{s}$ ) |
|-----------------------|-------------------------------------|-------------------------------------|----------|--------------------------|
| <b>7</b>              | 295 nm, 327 nm, 423 nm              | 613 nm                              | 0.26     | 1.34                     |
| <b>8</b>              | 319 nm, 354 nm, 414 nm              | 600 nm                              | 0.25     | 1.07                     |
| <b>9</b>              | 316 nm, 347 nm, 394 nm              | 576 nm                              | 0.21     | 1.44                     |
| <b>10</b>             | 354 nm, 399 nm, 456 nm              | 585 nm                              | 0.14     | 1.19                     |
| <b>11</b>             | 289 nm, 334 nm, 501 nm              |                                     |          |                          |
| protonated- <b>11</b> | 288 nm, 321 nm, 411 nm              | 602 nm                              | 0.09     | 0.48                     |
| <b>12</b>             | 325 nm, 383 nm, 493 nm              |                                     |          |                          |
| protonated- <b>12</b> | 314 nm, 380 nm, 450 nm              | 598 nm                              | <0.01    | 0.35                     |
| <b>13</b>             | 292 nm, 329 nm, 451 nm              |                                     |          |                          |
| protonated- <b>13</b> | 352 nm, 411 nm                      | 593 nm                              | 0.29     | 1.74                     |
| <b>14</b>             | 256 nm, 335 nm, 465 nm              |                                     |          |                          |
| protonated- <b>14</b> | 298 nm, 354 nm, 419 nm              | 607 nm                              | 0.18     | 1.30                     |
| <b>15</b>             | 288 nm, 336 nm, 475 nm              |                                     |          |                          |
| protonated- <b>15</b> | 324 nm, 354 nm, 420 nm              | 608 nm                              | 0.17     | 1.34                     |
| <b>16</b>             | 388 nm, 466 nm                      |                                     |          |                          |
| protonated- <b>16</b> | 353 nm, 372 nm, 418 nm              | 599 nm                              | 0.19     | 0.97                     |

<sup>a</sup>Emission spectra were measured by photoirradiation at 366 nm. <sup>b</sup> $\text{Ir}(\text{mpiq})_3$  **7** ( $\Phi = 0.26$  in toluene)<sup>13</sup> was used as the standard for the phosphorescence quantum yield measurement.

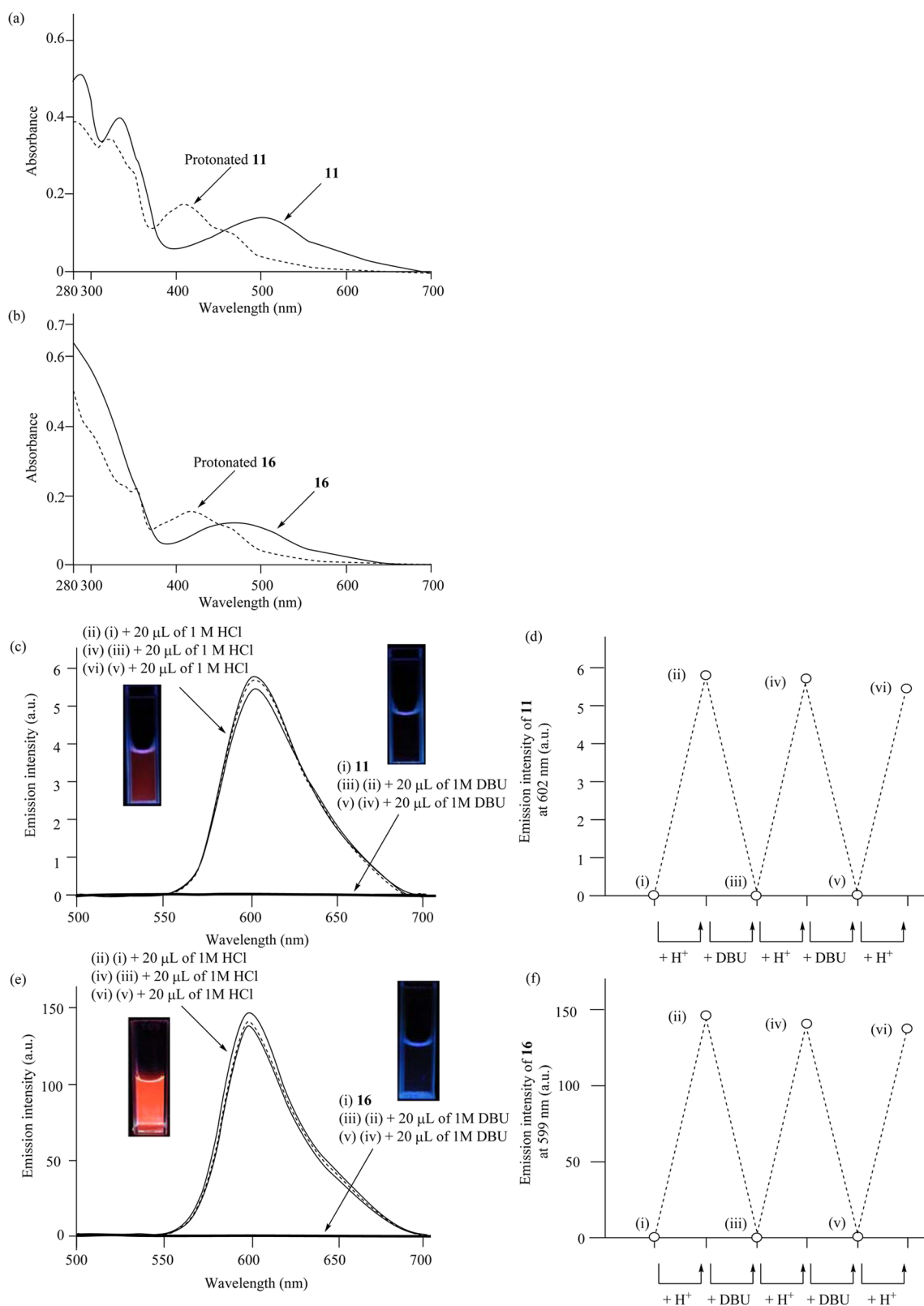


**Figure 2.** UV-vis spectra of **11** (a) and **16** (b) (10  $\mu\text{M}$ ) in DMSO at 25  $^{\circ}\text{C}$  before and after the addition of 1 M HCl in 1,4-dioxane. Change in emission spectra of **11** (c) and **16** (e) (10  $\mu\text{M}$ ) in degassed DMSO at 25  $^{\circ}\text{C}$  (excitation at 366 nm) upon the repeated addition of acid (1 M HCl in 1,4-dioxane) and base (1 M DBU in 1,4-dioxane). (i) **11** or **16** before addition of  $\text{H}^+$ , (ii) (i) + HCl, (iii) (ii) + DBU, (iv) (iii) + HCl, (v) (iv) + DBU, and (vi) (v) + HCl. Change in emission intensity of **11** at 602 nm (d) and **16** at 599 nm (f) caused by the repeated addition of HCl and DBU. [**11**] or [**16**] = 10  $\mu\text{M}$  and a.u. is in arbitrary units.

ca. 600 nm (red). When 1,8-diazabicyclo[5.4.0]undec-7-ene (DBU) was added to these solutions as a base, the red emission

was nearly completely quenched, and these processes proceeded in a reversible manner, as plotted in Figure 2d,f (excitation

spectra of deprotonated and protonated forms of **16** are shown in Figure S4 in Supporting Information). Almost the same behaviors were observed for **13**, **14**, and **15** (Figure S5 in Supporting Information). Note that emission intensity of protonated **11** ( $\Phi = 0.09$ ) and **12** ( $\Phi < 0.01$ ) are much weaker than that of **13**–**16** (Table 2).

The pH-dependent emission spectra of **11** and **13**–**16** (1–100  $\mu\text{M}$ ) in DMSO/100 mM buffer (1/6) are shown in Figure 3 and Figure S6 in Supporting Information. The

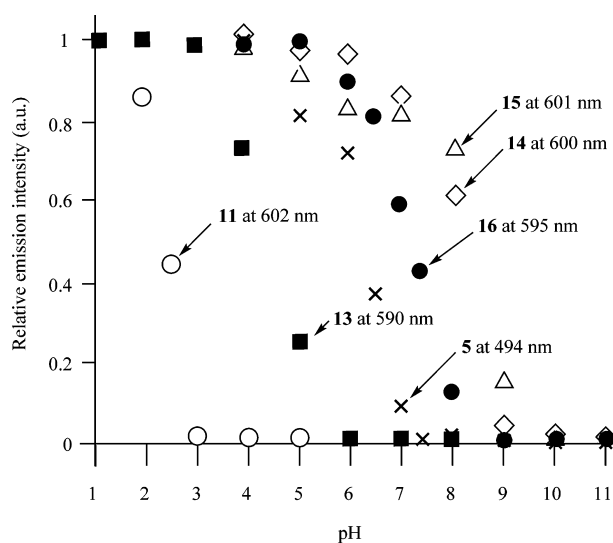


**Figure 3.** pH-Dependent change in emission intensity of **5** (1  $\mu\text{M}$ ) at 494 nm (x), **11** (100  $\mu\text{M}$ ) at 602 nm (o), **13** (1  $\mu\text{M}$ ) at 590 nm (■), **14** (10  $\mu\text{M}$ ) at 600 nm (◇), **15** (10  $\mu\text{M}$ ) at 601 nm (△) and **16** (10  $\mu\text{M}$ ) at 595 nm (●), in degassed DMSO/100 mM buffer (1/6, v/v). This relative emission intensity of **11** and **13** was calculated based on **1** at pH 1, and that of **5**, **14**, **15**, and **16** was calculated based on **1** at pH 4. Excitation at 366 nm; a.u. is in arbitrary units.

enhancement in emission intensity (at 602 nm) for **11** was observed at pH < 3, which is lower than that of **4** (pH 4–6) (Figure S6a).<sup>11a</sup> Note that the pK<sub>a</sub> value of the excited state of **11** (estimated by the pH-dependent change in emission) is close to that of its ground state (determined by UV–vis titration), as previously reported for **4**.<sup>11a,c</sup> It is assumed that the more extensive  $\pi$ -conjugation of the mpiq ligand and the more hydrophobic structure serve to decrease the pK<sub>a</sub> of **11** compared to **4**, which contains a tpy ligand. The introduction of diethylamino groups in **13** induced a shift in emission intensity threshold to ca. pH 4–5 from that of its original compound **11** (pH < 3) (Figure S6b). On the other hand, the pK<sub>a</sub> values of guanidine and iminoimidazolidine derivatives **14** and **15** were estimated to be >8, possibly due to the strong basicity of these basic groups (Figure 3 and Figure S6c and S6d in Supporting Information). Lastly, we found that the emission for **16** containing iminoimidazolidine and trifluoromethyl groups was enhanced at ~pH 7–8 (Figure 3 and Figure S6e; the predicted pK<sub>a</sub> values of the corresponding aniline derivatives are listed in Figure S1 in Supporting Information and change in UV–vis spectra of **16** at pH 4–11 is shown in Figure S7 in Supporting Information).<sup>23</sup> The photos in Figure 4 clearly show the pH-dependent behaviors of Ir(tpy)<sub>3</sub> derivatives **4** and **5** and Ir(mpiq)<sub>3</sub> derivatives **11**, **13**, **14**, **15**, and **16**. Note that the change in the emission of **5** and **16** occurs at almost the same pH range (Figure 4b,g).

**Density Functional Theory Calculations of 7–16.** Density functional theory (DFT) calculations of **7**–**16** were

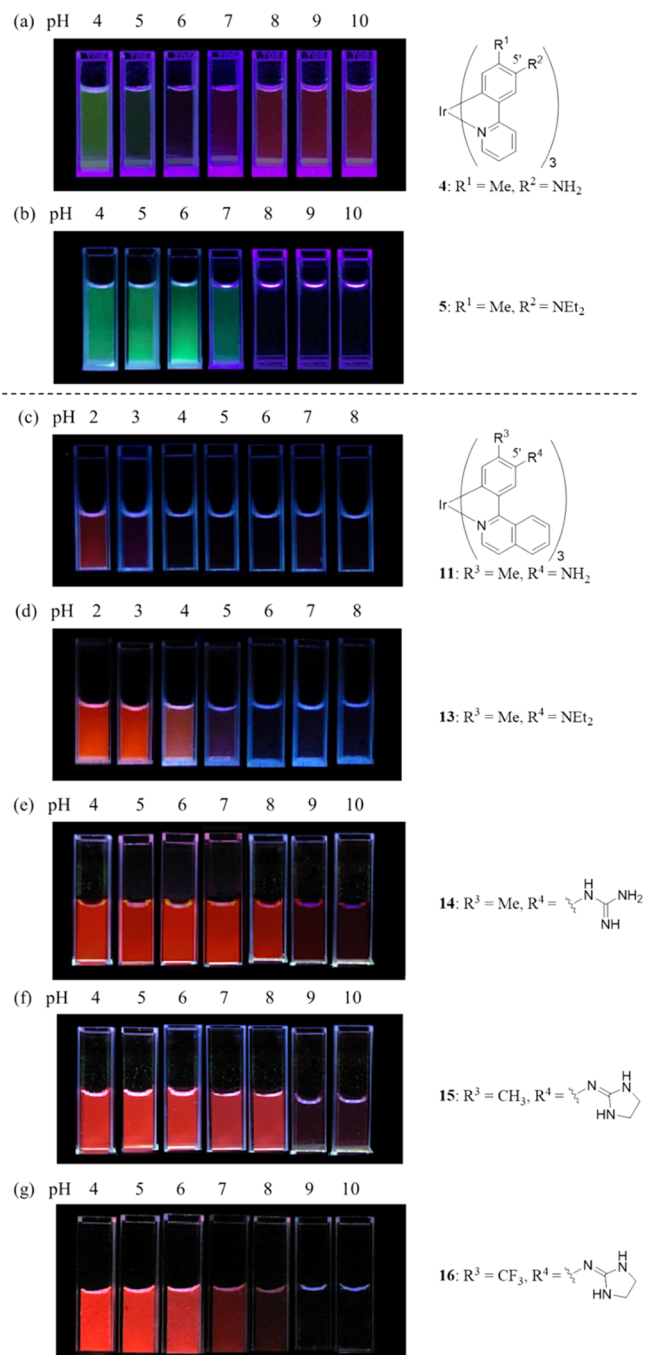


**Figure 4.** Photograph showing solutions of (a) **4** (100  $\mu\text{M}$ ), (b) **5** (1  $\mu\text{M}$ ), (c) **11** (50  $\mu\text{M}$ ), (d) **13** (1  $\mu\text{M}$ ), (d) **14** (10  $\mu\text{M}$ ), (f) **15** (10  $\mu\text{M}$ ), and (g) **16** (5  $\mu\text{M}$ ) in degassed DMSO/100 mM buffer (from pH 4 to 10) at 25 °C. Excitation at 365 nm.

performed using the Gaussian09 program, and the results are summarized in Figure S8 in Supporting Information with the results for **2** and **5**.<sup>14,15</sup> The B3LYP hybrid functional was used, together with the LanL2DZ basis set for the Ir atom and the 6-31G basis set for the H, C, F, N, and O atoms. The highest occupied molecular orbital–lowest unoccupied molecular orbital (HOMO–LUMO) shapes of the Ir(III) complexes **7**–**16** are almost similar, as shown in Figure 5. The HOMO orbital consists of phenyl(tolyl)- $\pi$  and Ir-d orbitals, while the LUMO orbital is mainly localized on the isoquinoline ring. Introduction of an electron-withdrawing group (a nitro group in **9** and **10**) stabilizes

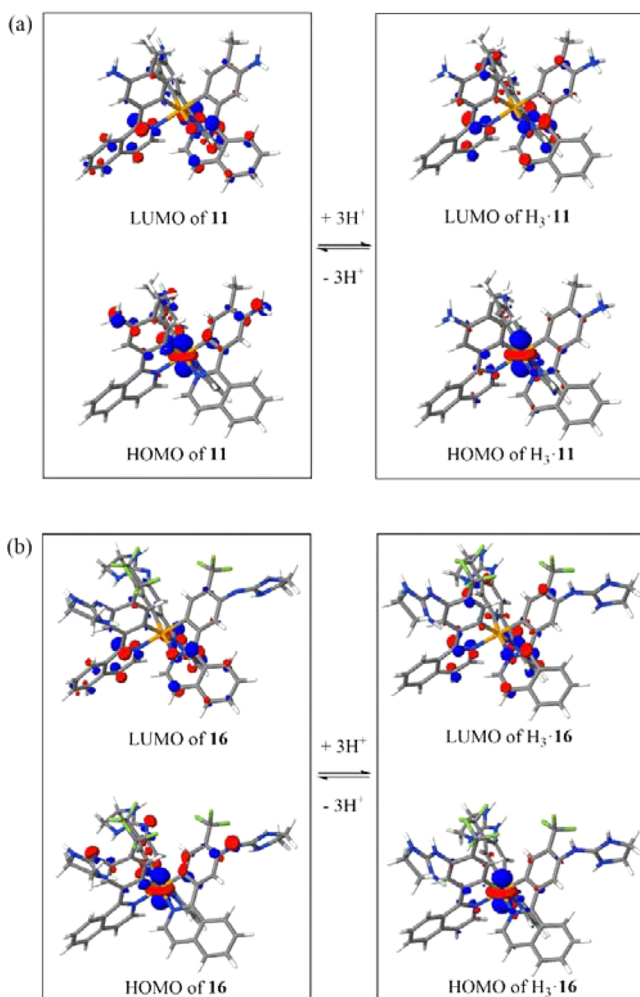


**Figure 5.** HOMO and LUMO surfaces of **11** and protonated·**11** (a) and **16** and protonated·**16** (b) calculated by DFT method using the B3LYP hybrid functional together with the LanL2DZ basis set for Ir atom and the 6-31G basis set for H, C, F, O, and N atoms.

both the HOMO and LUMO energy levels, resulting in an increase in the HOMO–LUMO energy gap of **9** ( $E_g = 3.27$  eV) and **10** ( $E_g = 3.21$  eV). This result may explain the blue shift in the emission wavelength (ca. 15–40 nm) of nitro derivatives **9** and **10**, as described below. On the other hand, an electron-donating group (amino group) induces destabilization of HOMO energy level to decrease in energy gap of **11** ( $E_g = 2.45$  eV), in comparison with that of **7** ( $E_g = 2.92$  eV) (Figure S8 in Supporting Information).

The HOMO and LUMO energy levels of the protonated and deprotonated forms of **11** and **16** are shown in Figure 6, and the results indicate that the HOMO–LUMO energy gaps are enhanced upon protonation of their amino groups. Similar behaviors were observed for our previous compounds, namely, **4**<sup>11a</sup> and **5**.<sup>11c</sup>

**Photophysical Properties of Nitro Derivatives 9 and 10.** UV–vis absorption and emission spectra of **9** and **10** in degassed DMSO at 25 °C are shown in Figure 7 with those for **7** and **8** (excitation at 366 nm). Note that the tris(nitro) derivatives **9** and **10** exhibit a rather strong orange-red color emission at 576 nm ( $\Phi = 0.21$ ) and 585 nm ( $\Phi = 0.14$ ), respectively, which are ca. 20 nm shorter than the corresponding values for **7** and **8** (Figure 7b,c). This is in agreement with the values for **24a**<sup>11a</sup> and **24b**<sup>24</sup> (Chart 4), the trinitro derivatives of **2** (Ir(tpy)<sub>3</sub>) and **3**

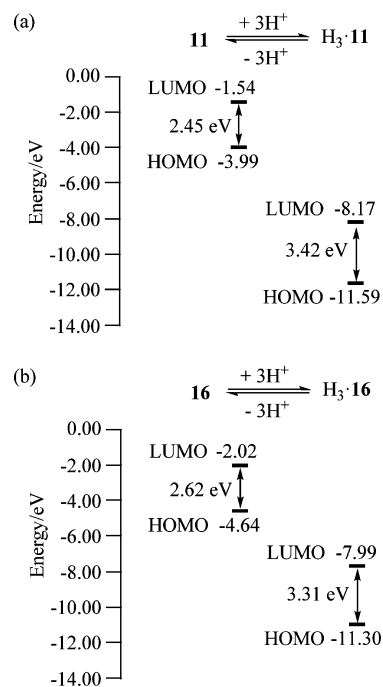


**Figure 6.** HOMO–LUMO energy gap of acid-free and protonated **11** (a) and **16** (b) calculated by DFT method using the B3LYP hybrid functional together with the LanL2DZ basis set for Ir atom and the 6-31G basis set for H, C, F, O, and N atoms.

(Ir(mppy)<sub>3</sub>), although the emission of **24a** and **24b** is very weak.<sup>25</sup> The luminescence lifetimes of complexes **9** and **10** were determined to be 1.44 and 1.19 μs, respectively, in DMSO at 25 °C (Table 2), supporting the conclusion that the emission occurs via excited triplet states. Generally, a nitro group functions as a strong quencher of luminescent dyes.<sup>26</sup> We assume that **9** and **10** are rare examples of the nitrated tris-cyclometalated Ir complexes that have strong emission properties.

To elucidate these phenomena, we performed DFT calculations of **2**, **24a**, and **9**, which afforded HOMO and LUMO orbitals presented in Figure 8. Generally, the HOMO orbital of tris(cyclometalated) Ir complexes such as **2** consists of phenyl-π and Ir-d orbitals, and its LUMO orbital is mainly localized on the pyridine ring (Figure 8a, left).<sup>4p</sup> As for **24a**, its LUMO orbital is localized on nitrophenyl parts (Figure 8b, left), implying that photoinduced intramolecular electron transfer occurs from the Ir center (HOMO) to the nitrophenyl units (LUMO), resulting in the quenching of the emission.<sup>26c</sup> In contrast, the LUMO of **9** is mainly localized on the isoquinoline rings and not on the nitrotolyl ring (Figure 8c, left). These data allowed us to conclude that strong emission of **9** and **10** results from the absence of LUMO on the nitrotolyl units of their ligand moieties.<sup>26c</sup>

**Live Cell Imaging of HeLa-S3 Cells Using 13–16 with MitoTracker and LysoTracker.** We previously reported that **5** is useful for the selective staining of lysosomes, an acidic organelle in cells in response to its pH.<sup>11c</sup> These data prompted us to perform luminescent imaging of living cells with the above-synthesized Ir complexes. After incubating HeLa-S3 cells in MEM/DMSO (pH 7.4, 95/5, v/v) with **13**, **15**, and **16** (50 μM) for 30 min at 37 °C and washing the cells with PBS, they were observed by confocal microscopy (Leica TCS SP2, Leica). Since the pH of lysosomes is lower than 5.5<sup>27</sup> and the pH of mitochondria is ~7.5,<sup>28</sup> costaining studies of these Ir complexes

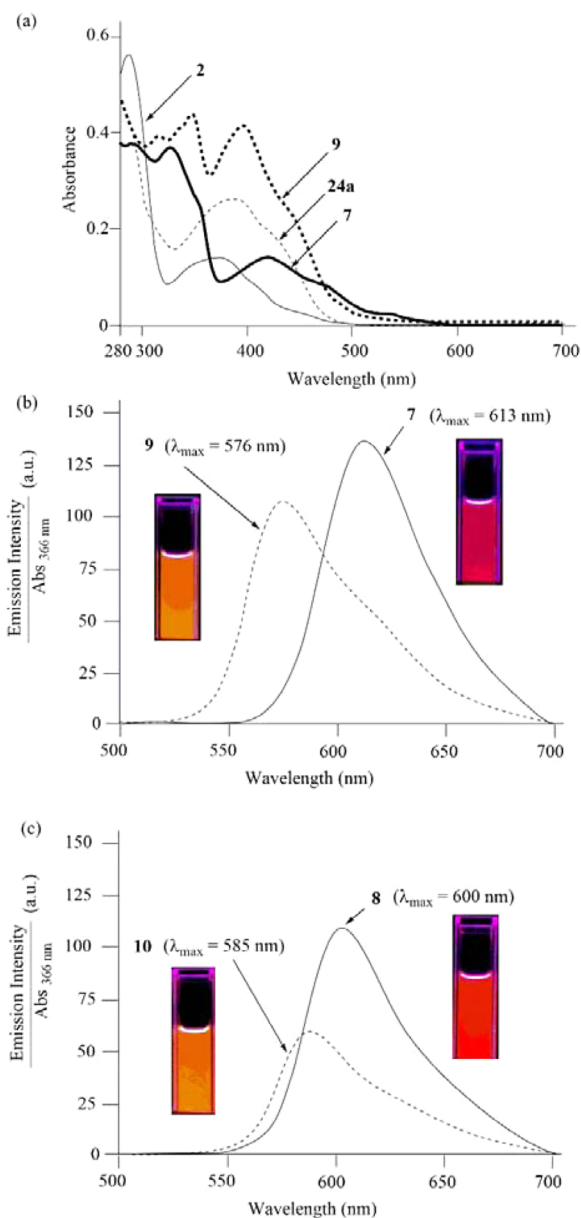
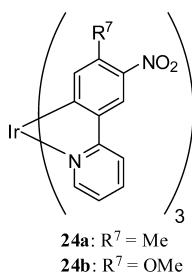


**Figure 7.** UV-vis spectra of **2** (plain curve), **24a** (plain and dashed curve), **7** (bold curve), and **9** (bold and dashed curve) (a). Emission spectra of **7** (plain curve) and **9** (plain and dashed curve) (b) and **8** (plain curve) and **10** (plain and dashed curve) (c) in DMSO at 25 °C. a.u. is in arbitrary units, and the intensity of emission was normalized with the absorbance of each compound at 366 nm, which was used for the excitation of the Ir complexes.  $[\text{Ir complex}] = 10 \mu\text{M}$ .

#### Chart 4



with a lysosomal dye (LysoTracker) and a mitochondrial dye (MitoTracker) were conducted.

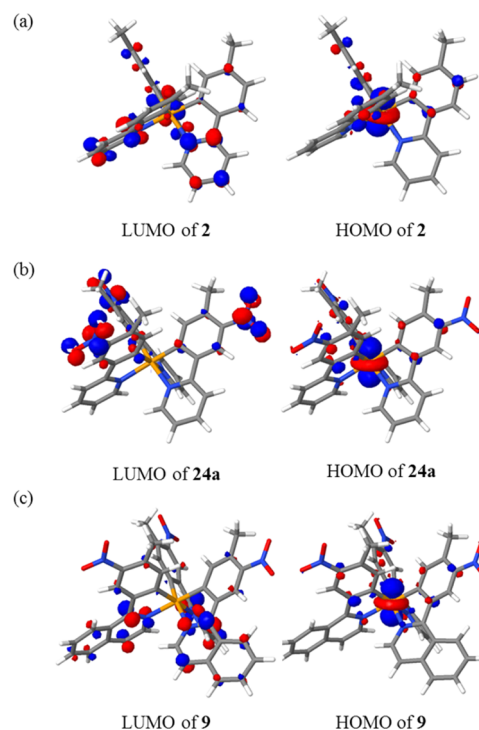


**Figure 8.** HOMOs and LUMOs of **2** (a), **24a** (b), and **9** (c), calculated by DFT method using the B3LYP hybrid functional together with the LanL2DZ basis set for Ir atom and the 6-31G basis set for H, C, O, and N atoms.

Figure 9 displays a typical bright field image, a luminescent image of Ir complexes, a luminescent image of MitoTracker Green or LysoTracker Green, and a merged image. For example, Figures 9a–d and 9e–h show the results for the costaining of HeLa-S3 cells with **13** and MitoTracker and LysoTracker, respectively. The cytotoxicity of these Ir complexes was very low at 50  $\mu\text{M}$  (data not shown). The emission area of **13** and MitoTracker and their merged image (Figure 9a–d) indicate that **13** is overlapped with MitoTracker to a negligible extent. In addition, the intracellular emission intensity of **13** is low probably due to its low  $\text{pK}_a$  value. On the other hand, the luminescent image with **13** and LysoTracker are largely overlapped (Figure 9e–h). The luminescent images of **14** or **15** are overlapped with both LysoTracker and MitoTracker, possibly due to their higher  $\text{pK}_a$  values (Figure 9i–p; the luminescent images with **14** are shown in Figure S9 in Supporting Information). The results of costaining studies of **16** and LysoTracker (Figure 9q–x) indicate that the emission area of **16** and LysoTracker are overlapped to a greater extent than those with MitoTracker. We therefore conclude that **16** is the optimal probe for the staining of lysosomes among red Ir complexes synthesized in this work.

It has been reported that CCCP inhibits oxidative phosphorylation,<sup>29</sup> decreases ATP production, and lowers the metabolic rate, resulting in the suppression of active transport.  $\text{NaN}_3$  is also known to function as a metabolic inhibitor.<sup>30</sup> As shown in Figure S10 in Supporting Information, the cellular uptake of **15** and **16** was not inhibited by CCCP (40  $\mu\text{M}$ ) nor  $\text{NaN}_3$  (5 mM) at 37 °C for 30 min in MEM/DMSO (95/5, v/v), indicating that **15** and **16** are taken up by cells via a passive transport mechanism. Although the intracellular concentrations of **13**–**16** in HeLa-S3 cells were measured by ICP-AES according to our previous method,<sup>11c</sup> these values were too low (<0.1 fmol/cell) to permit their detection.

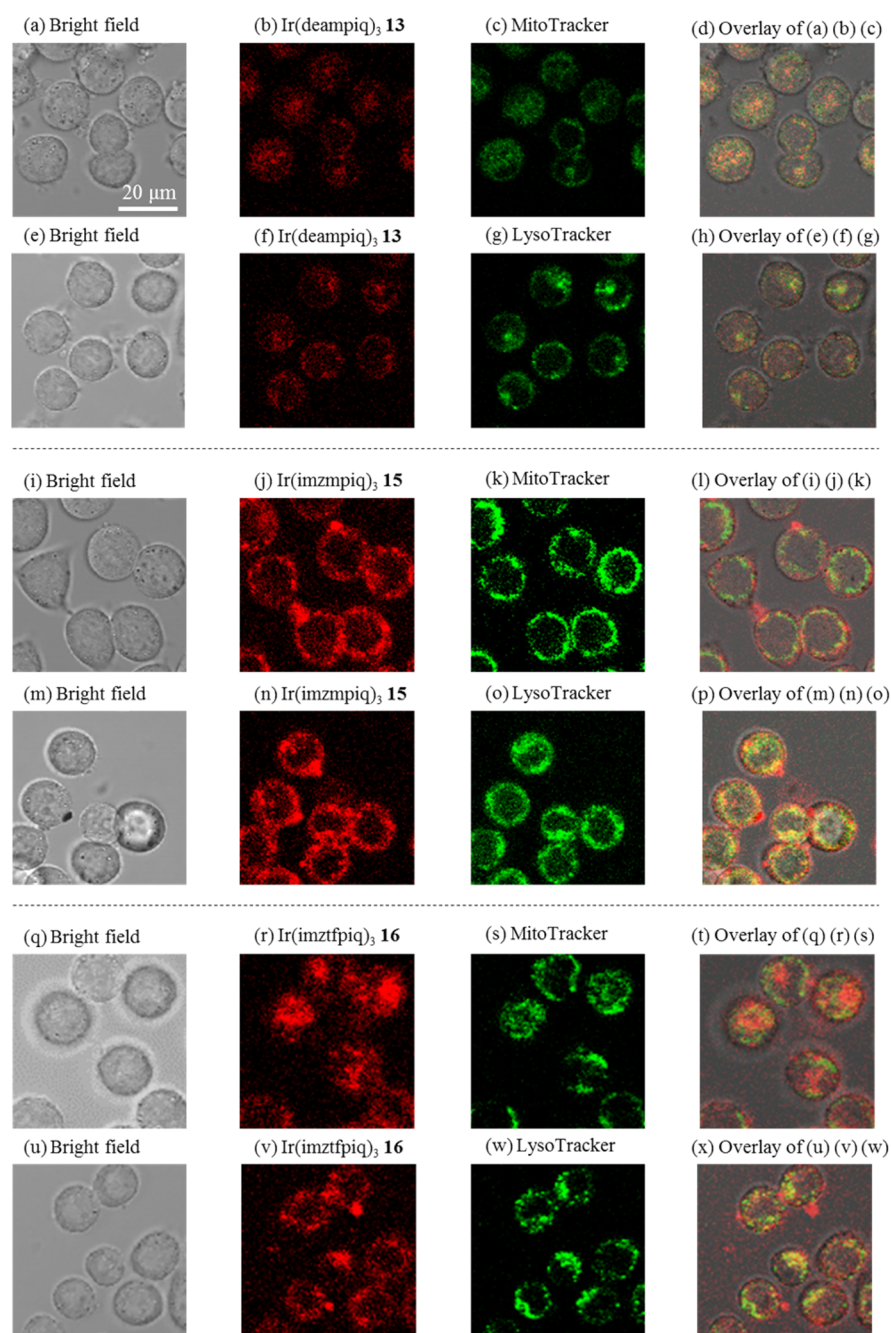


**Figure 9.** Luminescence microscope images (Leica TCS SP2, Leica) of HeLa-S3 cells stained with Ir complexes (50  $\mu$ M), MitoTracker Green (100 nM), or LysoTracker Green (500 nM) in MEM/DMSO (95/5, v/v) at 37  $^{\circ}$ C for 30 min. (a, e, i, m, q, and u) brightfield images of HeLa-S3, (b, f) emission images of **13**, (j, n) emission images of **15**, (r, v) emission images of **16**, (c, k, and s) emission images of MitoTracker Green, (g, o, and w) emission images of LysoTracker Green, (d) overlay image of (a–c), (h) overlay image of (e–g), (l) overlay image of (i–k), (p) overlay image of (m–o), (t) overlay image of (q–s), (x) overlay image of (u–w). Excitation at 350, 360, and 458 nm for Ir complexes and excitation at 488 nm for MitoTracker Green and LysoTracker Green.

### Generation of Singlet Oxygen by the Photoirradiation of Ir Complexes.

Ir complexes are known to function as photosensitizers for the production of singlet oxygen ( $^1\text{O}_2$ ) from triplet oxygen ( $^3\text{O}_2$ ) by photoirradiation.<sup>9</sup> We previously reported that the pH-dependent generation of  $^1\text{O}_2$  by photoirradiation of the Ir(III) complexes **5** and **6** and their application for inducing necrosis-like cell death of HeLa-S3 cells.<sup>11c,d</sup> These results allowed us to check the generation of  $^1\text{O}_2$  by the Ir complexes **13**, **14**, **15**, and **16** (10  $\mu$ M) in DMSO/H<sub>2</sub>O (3/2, v/v) upon photoirradiation at 470 nm, which is less toxic to living cells than UV light. The decomposition

of DPBF was monitored by the change in the UV–vis spectra, for which the absorbance at 415 nm decreases in the case of a reaction with  $^1\text{O}_2$ .<sup>31</sup> As shown in Figure 10, the protonated forms of **13**, **14**, **15**, and **16** (prepared in situ by addition of 0.01 M HCl aq) generate  $^1\text{O}_2$  more efficiently than their acid-free forms. Since these Ir complexes have an absorbance at longer wavelengths than that of **5** (Figure 2b in the text and Figure S3d–f in Supporting Information), the higher efficiency in  $^1\text{O}_2$  generation of **13**–**16** than those of **5** and protonated **5** can be explained by the fact that the absorbance of **13**–**16** at 470 nm is stronger than that for **5**.<sup>32</sup>

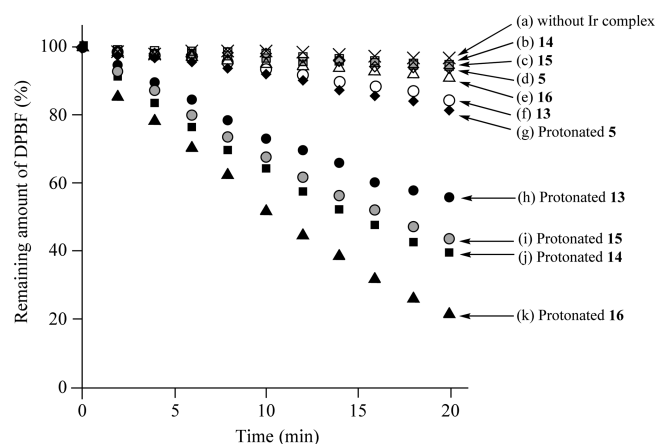


**Figure 10.** Photooxidation of DPBF ( $50 \mu\text{M}$ ) caused by photoirradiation of Ir complexes in  $\text{O}_2$ -aerated DMSO/ $\text{H}_2\text{O}$  (3/2 v/v), (a) blank in DMSO/ $\text{H}_2\text{O}$  (x), (b) 14 (□), (c) 15 (gray □), (d) 5 (◇), (e) 16 (△), (f) 13 (○), (g) protonated 5 (◆), (h) protonated 13 (●), (i) protonated 15 (gray ○), (j) protonated 14 (■) and (k) protonated 16 (▲) (excitation at 470 nm; FP-6200, JASCO). [5], [13], [14], [15], or [16] =  $10 \mu\text{M}$ . The protonated forms of Ir complexes were prepared in situ upon the addition of 0.01 M HCl aq. (final concentration:  $50 \mu\text{M}$  HCl).

The generation of  $^1\text{O}_2$  by the photoirradiation of acid-free 5 and 13 was examined using the ESR analysis of nitroxide radicals generated through the oxidation of the sterically hindered amines, 2,2,6,6-tetramethyl-4-piperidinol (4-hydroxy-TEMP) and TPC.<sup>11d,33</sup> As shown in Figure S12 in Supporting Information, the intensity of the ESR signal of the nitroxide radical of TPC generated by acid-free 5 and 13 is increased. In these experiments, the activity of the protonated forms of 5 and 13 was not determined, because TPC is protonated and is essentially unreactive for  $^1\text{O}_2$  under acidic conditions. Thus, we conclude that the photoirradiation of 5 and 13 facilitates the generation of  $^1\text{O}_2$  and that their protonated forms generate  $^1\text{O}_2$  more effectively than their acid-free forms (Figure 10 in the text and Figure S11 in Supporting Information).

**Induction of Cell Death of HeLa-S3 Cells upon Photoirradiation in the Presence of Ir Complexes.** We examined the photoinduced cell death of HeLa-S3 cells upon photoirradiation at 465 nm (Twinlight 465, Relyon, Japan) in the presence of the complexes 5, 13, 14, 15, and 16 by staining with PI, which exhibits strong red emission by intercalating with DNA in the nucleus because the nuclear membrane is damaged on necrotic cell death. Figure 11 shows a bright field image, a PI emission image, and an overlay image of the bright field and PI emission images in the absence and presence of Ir complexes after irradiation at 465 nm for 30 min. Negligible cell death was observed with photoirradiation in the absence of Ir complexes (Figure 11a–c) and no photoirradiation in the presence of 16 (Figure 11s–u and Figure 12). As shown in PI emission images obtained after the photoirradiation with Ir complexes (Figure 11e,h,k,n,q), a strong red emission from PI was observed, indicating that necrosis-like cell death was induced by photoirradiation of the Ir complexes (note that PI is excited at 540 nm, which scarcely excites Ir complexes). The lower cytotoxicity of 13 than that of 5 can be attributed to the lower intracellular concentration of its protonated form due to the lower  $\text{pK}_a$  value of diethylamino groups of 13 (see also Figure 12).

We also examined the inhibition of the induction of cell death by  $\text{NaN}_3$ , an inhibitor of  $^1\text{O}_2$  generation.<sup>9h</sup> As shown in Figure 13,

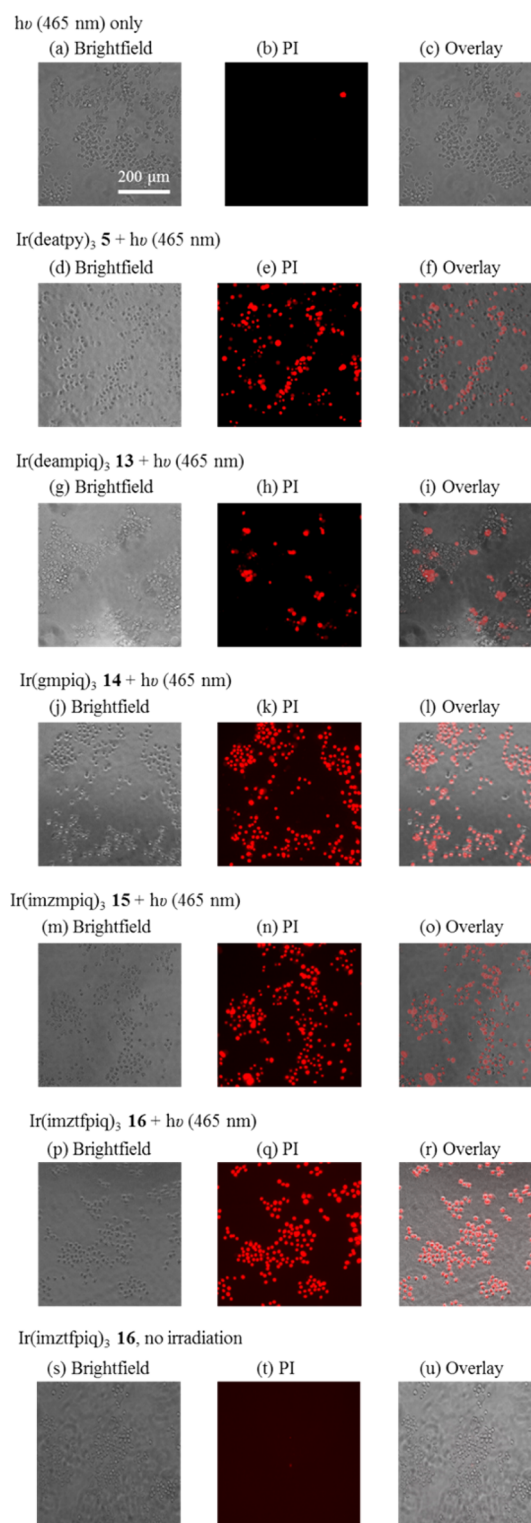


**Figure 11.** Luminescence microscope images (Biorevo BZ-9000, Keyence) of HeLa-S3 cells irradiated at 465 nm (Twinlight 465, Relyon) for 30 min with (a–c) only DMSO, (d–f) 5, (g–i) 13, (j–l) 14, (m–o) 15, and (p–r) 16 or (s–u) incubated for 30 min with 16 (no irradiation). After photoirradiation, the cells were incubated for 2 h again, and stained with PI ( $30 \mu\text{M}$ ) for 30 min. Excitation at 540 nm to observe PI. (a, d, g, j, m, p, and s) brightfield of HeLa-S3, (b, e, h, k, n, q, and t) emission images of PI, (c) overlay of (a, b), (f) overlay of (d, e), (i) overlay of (g, h), (l) overlay of (j, k), (o) overlay of (m, n), (r) overlay of (p, q), (u) overlay of (s, t).

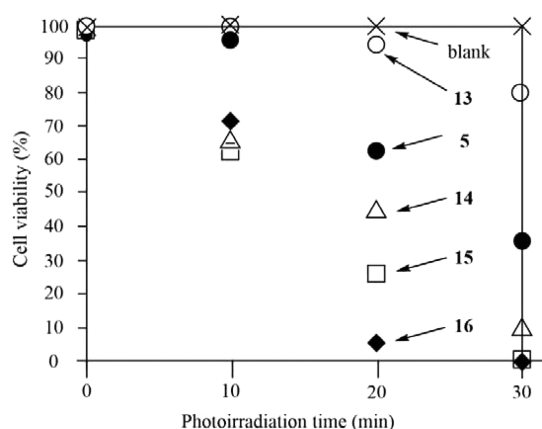


**Figure 12.** Change in cell viability of HeLa-S3 cells monitored by PI staining upon photoirradiation at 465 nm (Twinlight 465, Relyon) in the absence (×) and presence of **5** (10 μM) (●), **13** (10 μM) (○), **14** (10 μM) (△), **15** (10 μM) (□), and **16** (10 μM) (◆) in MEM/DMSO (99/1). Cell viability = (number of cells that were not stained by PI/number of all cells) × 100.

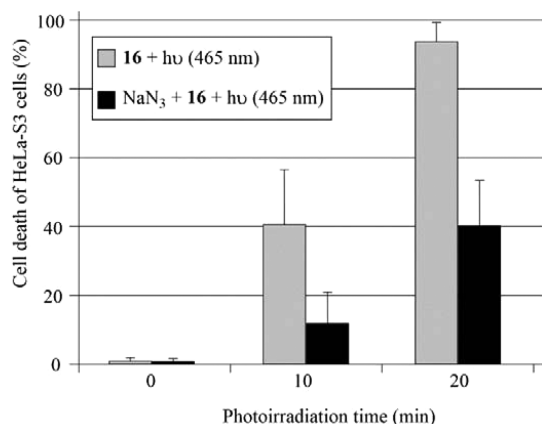


**Figure 13.** Cell death of HeLa-S3 cells upon photoirradiation at 465 nm (Twinlight 465, Relyon) with **16** (10 μM) in the absence (faded bar) and presence (filled bar) of NaN<sub>3</sub> (500 μM) in MEM/DMSO (99/1 v/v, monitored by PI staining). Cell death of HeLa-S3 cells (%) = (number of cells which were stained by PI/number of all cells) × 100.

NaN<sub>3</sub> inhibits the photoinduced cell death by **16**. Considering the fact that NaN<sub>3</sub> has little effect on the cellular uptake of Ir complexes (Figure S10 in Supporting Information), these findings suggest that cell death is triggered by <sup>1</sup>O<sub>2</sub>, which is generated by the excitation of the Ir complexes.

## CONCLUSIONS

In summary, we report on the synthesis, pH-dependent photochemical properties, cellular imaging, and photosensitizing activity of a series of new pH-activatable Ir(III) complexes **13**–**16**, based on the predicted pK<sub>a</sub> values of the corresponding aniline derivatives. These Ir complexes show a red emission, and their emission intensity is enhanced to a considerable extent upon the protonation of their basic groups in aqueous solution. It was found that the emission of **13** is nearly nonexistent at pH > 5, and a red emission is observed at pH < 5. In contrast, the guanidine and iminoimidazolidine derivatives **14** and **15** exhibit a strong emission at pH < 9, and the emission intensity of **16** having three CF<sub>3</sub> groups at the 4' position of the phenyl-isoquinoline ligand is increased at pH < 8. Moreover, Ir complexes

**14**–**16** are able to generate singlet oxygen (<sup>1</sup>O<sub>2</sub>) from triplet oxygen (<sup>3</sup>O<sub>2</sub>) more efficiently than **5** and **13** upon photoirradiation at 465 nm and induce the necrosis-like cell death of HeLa-S3 cells. Luminescence imaging studies of such complexes at acidic pH and the photoinduced cell death of cancer tissues using these Ir complexes are currently under way. It is of interest to note that the nitrated Ir complexes **9** and **10** exhibit a strong emission at 576–585 nm (an orange-red color), while the corresponding Ir(tpy)<sub>3</sub> and Ir(mppy)<sub>3</sub> counterparts, **24a** and **24b**, emit very weakly.

The results presented herein provide useful information for the future design and synthesis of new pH-activatable Ir complexes and their applications to photocatalytic reactions, photodynamic therapy, biological chemistry, medicinal chemistry, and related fields.

## ASSOCIATED CONTENT

### Supporting Information

Calculated pK<sub>a</sub> values of aniline derivatives, parameters for X-ray crystal structure analysis, crystal structure of **9**, UV–vis and excitation spectra, acid-induced changes in emission spectra, pH-dependent change in emission spectra, DFT-calculated HOMO–LUMO energy gap of Ir complexes, luminescence images of stained cells under microscope, photooxidation of DPBF, comparative photooxidation of TPC. The Supporting Information is available free of charge on the ACS Publications website at DOI: 10.1021/acs.inorgchem.5b00369. CCDC 1048292 contains the supplementary crystallographic data for the paper. These data can be obtained free of charge from The Cambridge Crystallographic Data Centre via [www.ccdc.cam.ac.uk/data\\_request/cif](http://www.ccdc.cam.ac.uk/data_request/cif).

## AUTHOR INFORMATION

### Corresponding Author

\*E-mail: [shinaoki@rs.noda.tus.ac.jp](mailto:shinaoki@rs.noda.tus.ac.jp).

### Notes

The authors declare no competing financial interest.

## ACKNOWLEDGMENTS

This work was supported by grants-in-aid from the Ministry of Education, Culture, Sports, Science and Technology (MEXT) of Japan (Nos. 22890200, 24890256, and 26860016 for Y.H. and Nos. 19659026, 22659055, 24659085, and 24640156 for S.A.), the Uehara Memorial Foundation for Y.H., and High-Tech Research Center Project for Private Universities (matching fund subsidy from MEXT). We appreciate Prof. H. Kawai (Faculty of Science, Tokyo Univ. of Science) for the measurement of phosphorescence quantum yield of Ir(III) complexes. We thank Prof. R. Abe and Dr. T. Suzuki (Research Institute for Biomedical Sciences, Tokyo Univ. of Science) for the helpful discussion and the preparation for the HeLa-S3 cells. We appreciate Mrs. F. Hasegawa (Faculty of Pharmaceutical Sciences, Tokyo Univ. of Science) for the measurement of mass spectra of Ir complexes and Ms. T. Matsuo (Research Institute of Sciences and Technology, Tokyo Univ. of Science) for the X-ray single-crystal structure analysis. We also appreciate Dr. K. Yoza (Bruker AXS) for helpful suggestions for the X-ray crystal structure analysis.

## REFERENCES

- (a) Han, J.; Burgess, K. *Chem. Rev.* **2010**, *110*, 2709–2728. (b) Hoogendoorn, S.; Blom, A. E. M.; Willems, L. I.; van der Marel, G. A.; Overkleeft, H. S. *Org. Lett.* **2011**, *13*, 5656–5659. (c) Hoogendoorn, S.; Habets, K. L.; Passemard, S.; Kuiper, J.; van der Marel, G. A.; Florea,

- B. I.; Overkleeft, H. S. *Chem. Commun.* **2011**, 47, 9363–9365. (d) Lee, H.; Akers, W.; Bhushan, K.; Bloch, S.; Sudlow, G.; Tang, R.; Achilefu, S. *Bioconjugate Chem.* **2011**, 22, 777–784. (e) Huang, R.; Yan, S.; Zheng, X.; Luo, F.; Deng, M.; Fu, B.; Xiao, Y.; Zhao, X.; Zhou, X. *Analyst* **2012**, 137, 4418–4420. (f) Kim, H. J.; Heo, C. H.; Kim, H. M. *J. Am. Chem. Soc.* **2013**, 135, 17969–17977. (g) Guo, Z.; Park, S.; Yoon, J.; Shin, I. *Chem. Soc. Rev.* **2014**, 43, 16–29. (h) Asanura, D.; Takaoka, Y.; Namiki, S.; Takikawa, K.; Kamiya, M.; Nagano, T.; Urano, Y.; Hirose, K. *Angew. Chem., Int. Ed.* **2014**, 53, 6085–6089. (i) Vegesna, G. K.; Janjanam, J.; Bi, J.; Luo, F.-T.; Zhang, J.; Olds, C.; Tiwari, A.; Liu, H. *J. Mater. Chem. B* **2014**, 2, 4500–4508. (j) Yin, J.; Hu, Y.; Yoon, J. *Chem. Soc. Rev.* in press, DOI: 10.1039/c4cs00275j.
- (2) Volk, T.; Jähde, E.; Fortmeyer, H. P.; Glüsenkamp, K.-H.; Rajewsky, M. F. *Br. J. Cancer.* **1993**, 68, 492–500.
- (3) Urano, Y.; Asanuma, D.; Hama, Y.; Koyama, Y.; Barrett, T.; Kamiya, M.; Nagano, T.; Watanabe, T.; Hasegawa, A.; Choyke, P. L.; Kobayashi, H. *Nat. Med.* **2009**, 15, 104–109.
- (4) (a) Dedeian, K.; Djurovich, P. I.; Garces, F. O.; Carlson, G.; Watts, R. J. *Inorg. Chem.* **1991**, 30, 1685–1687. (b) Lamansky, S.; Djurovich, P.; Murphy, D.; Abdel-Razzaq, F.; Kwong, R.; Tsyba, I.; Bortz, M.; Mui, B.; Bau, R.; Thompson, M. E. *Inorg. Chem.* **2001**, 40, 1704–1711. (c) Tamayo, A. B.; Alleyne, B. D.; Djurovich, P. I.; Lamansky, S.; Tsyba, I.; Ho, N. N.; Bau, R.; Thompson, M. E. *J. Am. Chem. Soc.* **2003**, 125, 7377–7387. (d) Lowry, M. S.; Hudson, W. R.; Pascal, R. A., Jr.; Bernhard, S. *J. Am. Chem. Soc.* **2004**, 126, 14129–14135. (e) Obara, S.; Itabashi, M.; Okuda, F.; Tamaki, S.; Tanabe, Y.; Ishii, Y.; Nozaki, K.; Haga, M. *Inorg. Chem.* **2006**, 45, 8907–8921. (f) Lowry, M. S.; Bernhard, S. *Chem.—Eur. J.* **2006**, 12, 7970–7977. (g) Evans, R. C.; Douglas, P.; Winscom, C. J. *Coord. Chem. Rev.* **2006**, 250, 2093–2126. (h) Flamigni, L.; Barbieri, A.; Sabatini, C.; Ventura, B.; Barigelletti, F. *Top. Curr. Chem.* **2007**, 281, 143–203. (i) Hedley, G. J.; Ruseckas, A.; Samuel, I. D. W. *Chem. Phys. Lett.* **2008**, 450, 292–296. (j) You, Y.; Park, S. Y. *Dalton Trans.* **2009**, 38, 1267–1282. (k) Wong, W.-Y.; Ho, C.-L. *Coord. Chem. Rev.* **2009**, 253, 1709–1758. (l) Wong, W.-Y.; Ho, C.-L. *J. Mater. Chem.* **2009**, 19, 4457–4482. (m) Ulbricht, C.; Beyer, B.; Friebe, C.; Winter, A.; Schubert, U. S. *Adv. Mater.* **2009**, 21, 4418–4441. (n) Chi, Y.; Chou, P.-T. *Chem. Soc. Rev.* **2010**, 39, 638–655. (o) Hofbeck, T.; Yersin, H. *Inorg. Chem.* **2010**, 49, 9290–9299. (p) You, Y.; Nam, W. *Chem. Soc. Rev.* **2012**, 41, 7061–7084.
- (5) (a) Baldo, M. A.; O'Brien, D. F.; You, Y.; Shoustikov, A.; Sibley, S.; Thompson, M. E.; Forrest, S. R. *Nature* **1998**, 395, 151–154. (b) Sasabe, H.; Kido, J. *Chem. Mater.* **2011**, 23, 621–630. (c) Farinola, G. M.; Ragni, R. *Chem. Soc. Rev.* **2011**, 40, 3467–3482.
- (6) (a) Goodall, W.; Williams, J. A. G. *J. Chem. Soc., Dalton Trans.* **2000**, 2893–2895. (b) Ho, M.-L.; Hwang, F.-M.; Chen, P.-N.; Hu, Y.-H.; Cheng, Y.-M.; Chen, K.-S.; Lee, G.-H.; Chi, Y.; Chou, P.-T. *Org. Biomol. Chem.* **2006**, 4, 98–103. (c) Konishi, K.; Yamaguchi, H.; Harada, A. *Chem. Lett.* **2006**, 35, 720–721. (d) Schmittle, M.; Lin, H. *Inorg. Chem.* **2007**, 46, 9139–9145. (e) Zhao, Q.; Cao, T.; Li, F.; Li, X.; Jing, H.; Yi, T.; Huang, C. *Organometallics* **2007**, 26, 2077–2081. (f) Zhao, Q.; Liu, S.; Shi, M.; Li, F.; Jing, H.; Yi, T.; Huang, C. *Organometallics* **2007**, 26, 5922–5930. (g) Zhao, N.; Wu, Y.-H.; Wen, H.-M.; Zhang, X.; Chen, Z.-N. *Organometallics* **2009**, 28, 5603–5611. (h) Zhao, Q.; Li, F.; Huang, C. *Chem. Soc. Rev.* **2010**, 39, 3007–3030. (i) Araya, J. C.; Gajardo, J.; Moya, S. A.; Aguirre, P.; Toupet, L.; Williams, J. A. G.; Escadellas, M.; Bozec, H. L.; Guerchais, V. *New J. Chem.* **2010**, 34, 21–24. (j) Brandel, J.; Sairenji, M.; Ichikawa, K.; Nabeshima, T. *Chem. Commun.* **2010**, 46, 3958–3960. (k) Guerchais, V.; Fillaut, J.-L. *Coord. Chem. Rev.* **2011**, 255, 2448–2457. (l) You, Y.; Han, Y.; Lee, Y.-M.; Park, S. Y.; Nam, W.; Lippard, S. J. *J. Am. Chem. Soc.* **2011**, 133, 11488–11491. (m) Qinghai, S.; Bats, J. W.; Schmittle, M. *Inorg. Chem.* **2011**, 50, 10531–10533. (n) Woo, H.; Cho, S.; Han, Y.; Chae, W.-S.; Ahn, D.-R.; You, Y.; Nam, W. *J. Am. Chem. Soc.* **2013**, 135, 4771–4787. (o) Lu, F.; Yamamura, M.; Nabeshima, T. *Dalton Trans.* **2013**, 42, 12093–12100. (p) Tang, Y.; Yang, H.-R.; Sun, H.-B.; Liu, S.-J.; Wang, J.-X.; Zhao, Q.; Liu, X.-M.; Xu, W.-J.; Li, S.-B.; Huang, W. *Chem.—Eur. J.* **2013**, 19, 1311–1319. (q) Ru, J.-X.; Guan, L.-P.; Tang, X.-L.; Dou, W.; Yao, X.; Chen, W.-M.; Liu, Y.-M.; Zhang, G.-L.; Liu, W.-S.; Meng, Y.; Wang, C.-M. *Inorg. Chem.* **2014**, 53, 11498–11506. (r) Ma, D.-L.; Chan, D. S.-H.; Leung, C.-H. *Acc. Chem. Res.* **2014**, 47, 3614–3631.
- (7) (a) Lo, K. K.-W.; Lee, P.-K.; Lau, J. S.-Y. *Organometallics* **2008**, 27, 2998–3006. (b) Zhang, K. Y.; Li, S. P.-Y.; Zhu, N.; Or, I. W.-S.; Cheung, M. S.-H.; Lam, Y.-W.; Lo, K. K.-W. *Inorg. Chem.* **2010**, 49, 2530–2540. (c) Leung, S.-K.; Kwok, K. Y.; Zhang, K. Y.; Lo, K. K.-W. *Inorg. Chem.* **2010**, 49, 4984–4995. (d) Zhang, K. Y.; Liu, H.-W.; Fong, T. T.-H.; Chen, X.-G.; Lo, K. K.-W. *Inorg. Chem.* **2010**, 49, 5432–5443. (e) Zhao, Q.; Yu, M.; Shi, L.; Liu, S.; Li, C.; Shi, M.; Zhou, Z.; Huang, C.; Li, F. *Organometallics* **2010**, 29, 1085–1091. (f) Lo, K. K.-W.; Li, S. P.-Y.; Zhang, K. Y. *New J. Chem.* **2011**, 35, 265–287. (g) Wu, H.; Yang, T.; Zhao, Q.; Zhou, J.; Li, C.; Li, F. *Dalton Trans.* **2011**, 40, 1969–1976. (h) Lee, P.-K.; Liu, H.-W.; Yiu, S.-M.; Louie, M.-W.; Lo, K. K.-W. *Dalton Trans.* **2011**, 40, 2180–2189. (i) Li, C.; Yu, M.; Sun, Y.; Wu, Y.; Huang, C.; Li, F. *J. Am. Chem. Soc.* **2011**, 133, 11231–11239. (j) You, Y.; Lee, S.; Kim, T.; Ohkubo, K.; Chae, W.-S.; Fukuzumi, S.; Jhon, G.-J.; Nam, W.; Lippard, S. J. *J. Am. Chem. Soc.* **2011**, 133, 18328–18342. (k) Lee, P.-K.; Law, W. H.-T.; Liu, H.-W.; Lo, K. K.-W. *Inorg. Chem.* **2011**, 50, 8570–8579. (l) Wu, Y.; Jing, H.; Dong, Z.; Zhao, Q.; Wu, H.; Li, F. *Inorg. Chem.* **2011**, 50, 7412–7420. (m) Baggaley, E.; Weinstein, J. A.; Williams, J. A. G. *Coord. Chem. Rev.* **2012**, 256, 1762–1785. (n) Murase, T.; Yoshihara, T.; Tobita, S. *Chem. Lett.* **2012**, 41, 262–263. (o) Yoshihara, T.; Yamaguchi, Y.; Hosaka, M.; Takeuchi, T.; Tobita, S. *Angew. Chem., Int. Ed.* **2012**, 51, 4148–4151. (p) Li, S. P.-Y.; Tang, T. S.-M.; Yiu, K. S.-M.; Lo, K. K.-W. *Chem.—Eur. J.* **2012**, 18, 13342–13354. (q) Lo, K. K.-W.; Chan, B. T.-N.; Liu, H.-W.; Zhang, K. Y.; Li, S. P.-Y.; Tang, T. S.-M. *Chem. Commun.* **2012**, 49, 4271–4273. (r) Lo, K. K.-W.; Zhang, K. Y. *RSC Adv.* **2012**, 2, 12069–12083. (s) You, Y. *Curr. Opin. Chem. Biol.* **2013**, 17, 699–707. (t) Cao, R.; Jia, J.; Ma, X.; Zhou, M.; Fei, H. *J. Med. Chem.* **2013**, 56, 3636–3644. (u) Zhou, Y.; Jia, J.; Li, W.; Fei, H.; Zhou, M. *Chem. Commun.* **2013**, 49, 3230–3232. (v) Law, W. H.-T.; Lee, L. C.-C.; Louie, M.-W.; Liu, H.-W.; Ang, T. W.-H.; Lo, K. K.-W. *Inorg. Chem.* **2014**, 52, 13029–13041. (w) Fan, Y.; Zhao, J.; Yan, Q.; Chen, P. R.; Zhao, D. *ACS Appl. Mater. Interfaces* **2014**, 6, 3122–3131. (x) Ma, X.; Jia, J.; Wang, X.; Fei, H. *J. Am. Chem. Soc.* **2014**, 136, 17734–17737. (y) Lo, K. K.-W.; Li, S. P.-Y. *RSC Adv.* **2014**, 24, 10560–10585. (z) Ma, D.-L.; He, H.-Z.; Zhong, H.-J.; Lin, S.; Chan, D. S.-H.; Wang, L.; Lee, S. M.-Y.; Leung, C.-H.; Wong, C.-Y. *ACS Appl. Mater. Interfaces* **2014**, 6, 14008–14015.
- (8) (a) Zhang, S.; Hosaka, M.; Yoshihara, T.; Negishi, K.; Iida, Y.; Tobita, S.; Takeuchi, T. *Cancer Res.* **2010**, 70, 4490–4498. (b) Yoshihara, T.; Kobayashi, A.; Oda, S.; Hosaka, M.; Takeuchi, T.; Tobita, S. *Proc. SPIE* **2012**, 8233, 82330A1–82330A8.
- (9) (a) Gao, R.; Ho, D. G.; Hernandez, B.; Selke, M.; Murphy, D.; Djurovich, P. I.; Thompson, M. E. *J. Am. Chem. Soc.* **2002**, 124, 14828–14829. (b) Djurovich, P. I.; Murphy, D.; Thompson, M. E.; Hernandez, B.; Gao, R.; Hunt, P. L.; Selke, M. *Dalton Trans.* **2007**, 34, 3763–3770. (c) Takizawa, S.; Aboshi, R.; Murata, S. *Photochem. Photobiol. Sci.* **2011**, 10, 895–903. (d) Sun, J.; Zhao, J.; Guo, H.; Wu, W. *Chem. Commun.* **2012**, 48, 4169–4171. (e) Li, S. P.-Y.; Lau, C. T.-S.; Louie, M.-W.; Lam, Y.-W.; Lo, K. K.-W. *Biomaterials* **2013**, 34, 7519–7532. (f) Ashen-Garry, D.; Selke, M. *Photochem. Photobiol.* **2014**, 90, 257–274. (g) Ye, R.-R.; Tan, C.-P.; He, L.; Chen, M.-H.; Ji, L.-N.; Mao, Z.-W. *Chem. Commun.* **2014**, 50, 10945–10948. (h) Xue, F.; Lu, Y.; Zhou, Z.; Shi, M.; Yan, Y.; Yang, H.; Yang, S. *Organometallics* **2015**, 34, 73–77. (i) Maggioni, D.; Galli, M.; D'Alfonso, L.; Inverso, D.; Dozzi, M. V.; Sironi, L.; Iannaccone, M.; Collini, M.; Ferruti, P.; Ranucci, E.; D'Alfonso, G. *Inorg. Chem.* **2015**, 54, 544–553.
- (10) (a) Licini, M.; Williams, J. A. G. *Chem. Commun.* **1999**, 1943–1944. (b) Arm, K. J.; Leslie, W.; Williams, J. A. G. *Inorg. Chim. Acta* **2006**, 359, 1222–1232. (c) Murphy, L.; Congreve, A.; Palsson, L.-O.; Williams, J. A. G. *Chem. Commun.* **2010**, 46, 8743–8745. (d) Chen, Y.; Zhang, A.; Liu, Y.; Wang, K. J. *Organomet. Chem.* **2011**, 696, 1716–1722. (e) Goldstein, D. C.; Cheng, Y. Y.; Schmidt, T. W.; Bhadbbhade, M.; Thordarson, P. *Dalton Trans.* **2011**, 40, 2053–2061. (f) Weng, J.; Mei, Q.; Jiang, W.; Fan, Q.; Tong, B.; Ling, Q.; Huang, W. *Analyst* **2013**, 138, 1689–1699. (g) He, L.; Tan, C.-P.; Ye, R.-R.; Zhao, Y.-Z.; Liu, Y.-H.; Zhao, Q.; Ji, L.-N.; Mao, Z.-W. *Angew. Chem., Int. Ed.* **2014**, 53, 12137–12141. (h) Zhang, Q.; Zhou, M. *Talanta* **2015**, 131, 666–671.

- (11) (a) Aoki, S.; Matsuo, Y.; Ogura, S.; Ohwada, H.; Hisamatsu, Y.; Moromizato, S.; Shiro, M.; Kitamura, M. *Inorg. Chem.* **2011**, *50*, 806–818. (b) Hisamatsu, Y.; Aoki, S. *Eur. J. Inorg. Chem.* **2011**, 5360–5369. (c) Moromizato, S.; Hisamatsu, Y.; Suzuki, T.; Matsuo, Y.; Abe, R.; Aoki, S. *Inorg. Chem.* **2012**, *51*, 12697–12706. (d) Nakagawa, A.; Hisamatsu, Y.; Moromizato, S.; Kohno, M.; Aoki, S. *Inorg. Chem.* **2014**, *53*, 409–422. (e) Hisamatsu, Y.; Shibuya, A.; Suzuki, N.; Suzuki, T.; Abe, R.; Aoki, S. *Bioconjugate Chem.* in press, DOI: 10.1021/acs.bioconjchem.5b00095.
- (12) For the other examples of the substitution reactions of cyclometalated complexes, see: (a) Cheung, K.-M.; Zhang, Q.-F.; Chan, K.-W.; Lam, M. H. W.; Williams, I. D.; Leung, W.-H. *J. Organomet. Chem.* **2005**, *690*, 2913–2921. (b) Gagliardo, M.; Snelders, D. J. M.; Chase, P. A.; Klein Gebbink, R. J. M.; van Klink, G. P. M.; van Koten, G. *Angew. Chem., Int. Ed.* **2007**, *46*, 8558–8573. (c) Qin, T.; Ding, J.; Wang, L.; Baumgarten, M.; Zhou, G.; Mullen, K. *J. Am. Chem. Soc.* **2009**, *131*, 14329–14336.
- (13) (a) Tsuboyama, A.; Iwawaki, H.; Furugori, M.; Mukaide, T.; Kamatani, J.; Igawa, S.; Moriyama, T.; Miura, S.; Takiguchi, T.; Okada, S.; Hoshino, M.; Ueno, K. *J. Am. Chem. Soc.* **2003**, *125*, 12971–12979. (b) Okada, S.; Okinaka, K.; Iwawaki, H.; Furugori, M.; Hashimoto, M.; Mukaide, T.; Kamatani, J.; Igawa, S.; Tsuboyama, A.; Takiguchi, T.; Ueno, K. *Dalton Trans.* **2005**, *9*, 1583–1590.
- (14) Frisch, M. J.; Trucks, G. W.; Schlegel, H. B.; Scuseria, G. E.; Robb, M. A.; Cheeseman, J. R.; Scalmani, G.; Barone, V.; Mennucci, B.; Petersson, G. A.; Nakatsuji, H.; Caricato, M.; Li, X.; Hratchian, H. P.; Izmaylov, A. F.; Bloino, J.; Zheng, G.; Sonnenberg, J. L.; Hada, M.; Ehara, M.; Toyota, K.; Fukuda, R.; Hasegawa, J.; Ishida, M.; Nakajima, T.; Honda, Y.; Kitao, O.; Nakai, H.; Vreven, T.; Montgomery, J. A., Jr.; Peralta, J. E.; Ogliaro, F.; Bearpark, M.; Heyd, J. J.; Brothers, E.; Kudin, K. N.; Staroverov, V. N.; Kobayashi, R.; Normand, J.; Raghavachari, K.; Rendell, A.; Burant, J. C.; Iyengar, S. S.; Tomasi, J.; Cossi, M.; Rega, N.; Millam, M. J.; Klene, M.; Knox, J. E.; Cross, J. B.; Bakken, V.; Adamo, C.; Jaramillo, J.; Gomperts, R.; Stratmann, R. E.; Yazyev, O.; Austin, A. J.; Cammi, R.; Pomelli, C.; Ochterski, J. W.; Martin, R. L.; Morokuma, K.; Zakrzewski, V. G.; Voth, G. A.; Salvador, P.; Dannenberg, J. J.; Dapprich, S.; Daniels, A. D.; Farkas, Ö.; Foresman, J. B.; Ortiz, J. V.; Cioslowski, J.; Fox, D. J. *Gaussian 09*, Revision D.01; Gaussian, Inc.: Wallingford, CT, 2009.
- (15) (a) Hay, P. J. *J. Phys. Chem. A* **2002**, *106*, 1634–1641. (b) Fantacci, S.; Angelis, F. D. *Coord. Chem. Rev.* **2011**, *255*, 2704–2726.
- (16) Guo, Z.-X.; Cammidge, A. N.; Horwell, D. C. *Tetrahedron Lett.* **2000**, *56*, 5169–5175.
- (17) Tian, Z.; Edwards, P.; Roeske, R. W. *Int. J. Peptide Protein Res.* **1992**, *40*, 119–126.
- (18) Helgen, C.; Bochet, C. G. *J. Org. Chem.* **2003**, *68*, 2483–2486.
- (19) (a) O'Donovan, D. H.; Rozas, I. *Tetrahedron Lett.* **2012**, *53*, 4532–4535. (b) Rodriguez, F.; Rozas, I.; Ortega, J. E.; Erdozain, A. M.; Meana, J. J.; Callado, L. F. *J. Med. Chem.* **2008**, *51*, 3304–3312.
- (20) (a) Hatchard, C. G.; Parker, C. A. *Proc. R. Soc. London, Ser. A* **1956**, *235*, 518–536. (b) Murov, S. L.; Carmichael, I.; Hug, G. L. *Handbook of Photochemistry*, 2nd ed.; Marcel Dekker: New York, 1993.
- (21) Konno, H.; Sasaki, Y. *Chem. Lett.* **2003**, *32*, 252–253.
- (22) The average N(mpiq-NO<sub>2</sub>)-Ir and C(mpiq-NO<sub>2</sub>)-Ir bond distances of **9** are 2.14 Å and 1.99 Å (Figure S2a in Supporting Information), which are almost same as those of **25a** and **25b** shown in Figure S2b (ref 13a) and **26** shown in Figure S2c in Supporting Information (ref 11a). As shown in Figure S2a, the dihedral angles between the nitro and tolyl groups are 13.9°–27.0°, indicating that the three nitro groups have a twisted conformation with respect to the tolyl rings and the dihedral angles between the isoquinoline and tolyl ring of **9** are ca. 16.6° (average value of 13.5°, 16.5°, and 19.7°), possibly due to steric interactions between the H<sub>a</sub> in the tolyl ring and the H<sub>b</sub> in the isoquinoline ring. This later value is smaller than the corresponding values for **25a** (ca. 22.9°) and **25b** (ca. 19.9°), although the C1–C1' bond connecting the tolyl and isoquinoline rings is almost the same as those of **9**, **25a**, **25b**, and **26** (1.48 Å~1.49 Å). One of the reasons for the smaller H<sub>a</sub>–H<sub>b</sub> conflict in **9** can be attributed to the greater C1–C1'–C6' bond angle of **9** (ca. 125.9°) compare to that for **25a** (ca. 123.4°).
- (23) The pH-dependent change in UV–vis spectra of **16** is displayed in Figure S7 in Supporting Information.
- (24) Hisamatsu, Y.; Aoki, S. Details will be reported elsewhere.
- (25) It has been reported that a heteroleptic Ir complex with nitro group exhibits a weak emission ( $\Phi < 0.01$ ). See: (a) Kappaun, S.; Sax, S.; Eder, S.; Möller, K. C.; Waich, K.; Niedermair, F.; Saf, R.; Mereiter, K.; Jacob, J.; Müllen, K.; List, E. J. W.; Slugovc, C. *Chem. Mater.* **2007**, *19*, 1209–1211. (b) Agarwal, N.; Nayak, P. K. *Tetrahedron Lett.* **2008**, *49*, 2710–2713. (c) Davies, D. L.; Lowe, M. P.; Ryder, K. S.; Singh, K.; Singh, S. *Dalton Trans.* **2011**, 1028–1030.
- (26) (a) Munkholm, C.; Parkinson, D.-R.; Walt, D. R. *J. Am. Chem. Soc.* **1990**, *112*, 2608–2612. (b) Ueno, T.; Urano, Y.; Kojima, H.; Nagano, T. *J. Am. Chem. Soc.* **2006**, *128*, 10640–10641. (c) Takeno, K.; Ogawa, R.; Sakamoto, R.; Tsuchiya, M.; Otani, T.; Saito, T. *Org. Lett.* **2014**, *16*, 3212–3215.
- (27) Demaurex, N. *News Physiol. Sci.* **2002**, *17*, 1–5.
- (28) Orij, R.; Postmus, J.; Beek, A. T.; Brul, S.; Smits, G. J. *Microbiology* **2009**, *155*, 268–278.
- (29) (a) Poole, B.; Ohkuma, S. *J. Cell Biol.* **1981**, *90*, 665–669. (b) Demaurex, N.; Furuya, W.; D'Souza, S.; Bonifacino, J. S.; Grinstein, S. *J. Biol. Chem.* **1998**, *273*, 2044–2051. (c) Lau, J. S.-Y.; Lee, P.-K.; Tsang, K. H.-K.; Ng, C. H.-C.; Lam, Y.-W.; Cheng, S.-H.; Lo, K. K.-W. *Inorg. Chem.* **2009**, *48*, 708–718.
- (30) Gillaud, M.; Russier, J.; Bianco, A. *J. Am. Chem. Soc.* **2014**, *136*, 810–819.
- (31) (a) Howard, J. A.; Mendenhall, G. D. *Can. J. Chem.* **1975**, *53*, 2199–2201. (b) Gorman, A.; Killoran, J.; O'Shea, C.; Kenna, T.; Gallagher, W. M.; O'Shea, D. F. *J. Am. Chem. Soc.* **2004**, *126*, 10619–10631. (c) McDonnell, S. O.; Hall, M. J.; Allen, L. T.; Byrne, A.; Gallagher, W. M.; O'Shea, D. F. *J. Am. Chem. Soc.* **2005**, *127*, 16360–16361.
- (32) We measured the <sup>1</sup>O<sub>2</sub> generation of **5**, **13**, **14**, **15**, and **16** and their protonated forms upon photoirradiation at ca. 370 nm, at which absorption of these Ir complexes is almost identical. The results indicate that the efficiency of protonated **5** is comparable to those of protonated **13**, **14**, **15**, and **16** as shown in Figure S11 in Supporting Information.
- (33) Nakamura, K.; Ishiyama, K.; Ikai, H.; Kanno, T.; Sasaki, K.; Niwano, Y.; Kohno, M. *J. Clin. Biochem. Nutr.* **2011**, *49*, 87–95.